

Introduction to Astrophysics and Cosmology

The Thermal history of the Universe

Helga Dénés 2024 S1 Yachay Tech

hdenes@yachaytech.edu.ec

The horizon problem and inflation

Since the Universe began with a violent Big Bang, it is **very unlikely that the Universe was created as a very homogeneous system**. **Why then is the Universe so homogeneous now?**

Suppose **inhomogeneities** are suddenly created **inside a gas kept within a container**. We expect that the gas from regions of higher density will move to regions of lower density to establish homogeneity again.

If c_s is the sound speed, we expect that regions of size $c_s t$ will **become homogeneous in time t** .

At the present time when the age of the Universe is t , we **could not have received information from regions further away than ct** because any information starting from those regions beyond ct would not be able to reach us by today. Hence **a sphere of radius ct around us is our *horizon***. We **can have causal contacts only with regions inside this horizon**. We may expect the Universe to have become **homogeneous over regions of horizon size, but not over larger regions**.

There is enough **evidence to show that the Universe is actually homogeneous over regions much larger than the horizon**.

The horizon problem and inflation

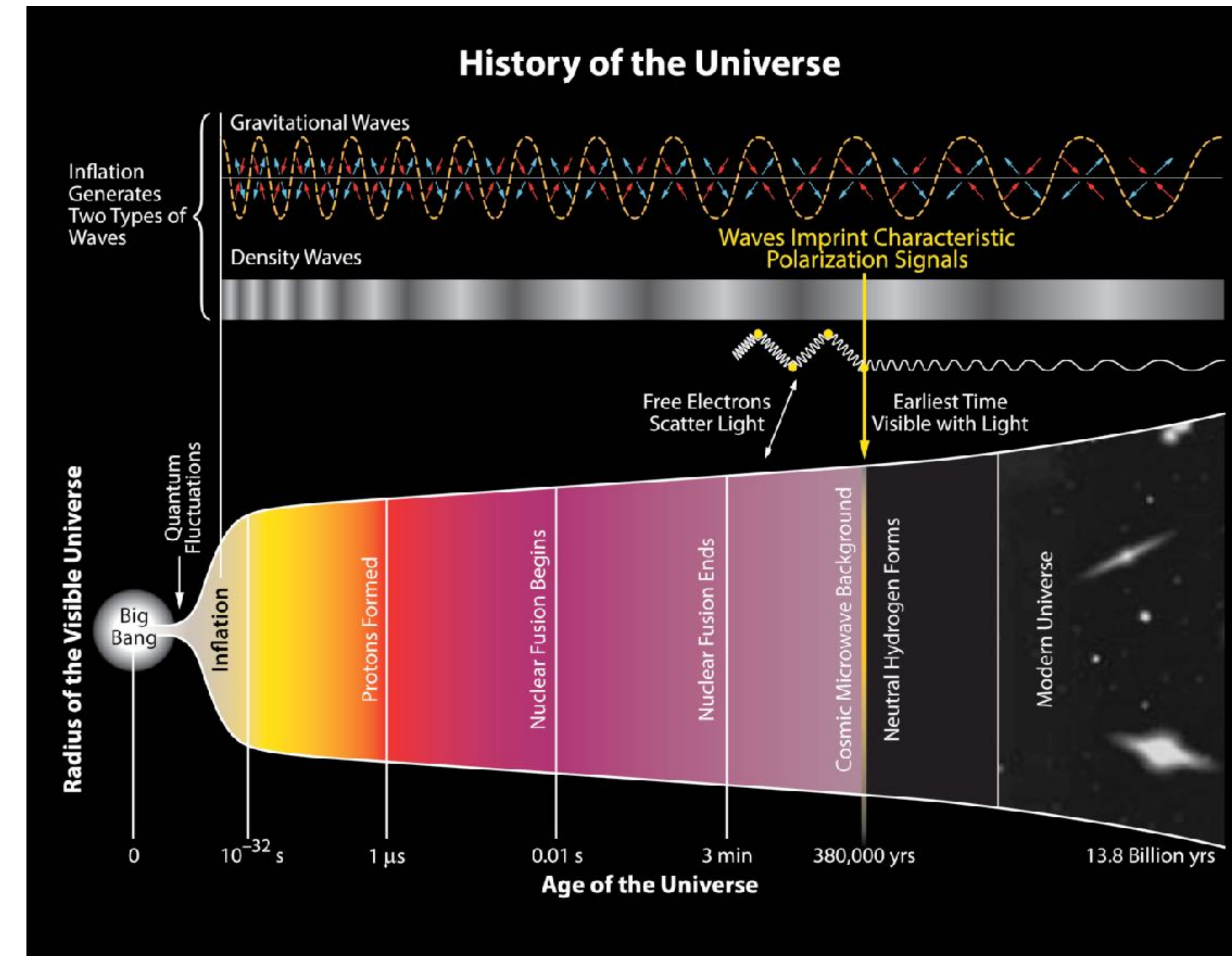
Photons in the CMBR reach us after travelling through space for time comparable to the age of the Universe.

Consider CMBR photons coming from two diametrically opposite regions in the sky. These two regions are causally **connected to us**, **but are not causally connected to each other** because the information from one of the regions had just time enough to reach us and did not yet have time to reach the other region. **The isotropy of CMBR, however, suggests that these two regions** which apparently had never been in causal contact **have the same physical characteristics**, since they produce CMBR of exactly the same nature. How is it possible that regions which are out of each other's horizons and which have never been in causal contact are so homogeneous? **This is known as the *horizon problem* in cosmology.**

Guth proposed a solution to the horizon problem. On the basis of some field theoretic arguments which are beyond the scope of this book, **Guth suggested that there was a brief phase in the very early Universe when the Universe expanded very rapidly and became larger by several orders of magnitude**. This is **called *inflation***. If this is true, then **the Universe before inflation must have been much, much smaller than what we would expect it to be if inflation had not taken place**. **Different parts of the Universe could have been causally connected** if the Universe was very small before inflation and thereby the homogeneity of the Universe could have been established.

The horizon problem and inflation

Illustration of the history of the Universe. The upper part of the figure illustrates what signatures we expect from the Inflation period → gravitational waves and density waves.



Baryons

$$\eta = \frac{n_{B,0}}{n_{\gamma,0}} = 2.73 \times 10^{-8} \Omega_{B,0} h^2. \quad (11.19)$$

The photon number density $n_{\gamma,0}$ is nearly eight orders of magnitude larger than the baryon number density $n_{B,0}$. As long as new photons or baryons are not created, both these numbers fall as a^{-3} and their ratio does not change. Even at the time when photons decoupled from matter, this ratio must have had this value. **Why are there many more photons than baryons?**

In the early Universe when the temperature was **higher than a few GeV** and **baryon-antibaryon pairs could be formed**, the number of either baryons or antibaryons would have been **comparable to the number of photons**, since all these numbers would have been given by (11.9). But **the number of baryons must have been slightly larger than the number of antibaryons to ensure that some baryons were left over** after the **baryon-antibaryon annihilation** which must have taken place when the temperature fell below GeV.

If Δn_B was the excess in the number density of baryons compared to the number density of antibaryons before the annihilation, then we must have

$$\frac{\Delta n_B}{n_B} \approx 10^{-8} \quad (11.33)$$

if we want the baryon-to-photon ratio to have a value like this after annihilation.

Baryons

Many physicists feel that it is **esthetically more satisfying to assume that the Universe was created with equal numbers of baryons and antibaryons** rather than to assume that the Universe was created with such a tiny imbalance.

If the Universe really had equal numbers of baryons and antibaryons in the beginning, then the net baryon number Δn_B was **initially zero and it had to change to a non-zero value later**.

We find the baryon number to be a conserved quantity in all particle interactions we study at the present time.

If the Universe was created with equal numbers of baryons and antibaryons, then the small excess of baryons over antibaryons could arise only if **baryon number conservation was violated in the very early Universe**. This is **known as the problem of *baryogenesis*** and has been of some interest to theoretical particle physicists.

The formation of atoms

Let's look at some of the later landmarks in that evolutionary history. After the **electron-positron annihilation** discussed, the Universe consisted of the **basic constituents of ordinary matter – protons, helium nuclei and electrons** – in addition to **the non-baryonic matter and the relativistic particles** (photons and neutrinos).

We have seen that the Universe became **matter-dominated** when its size was $1 + z = 2.3 \times 10^4 \Omega_{M,0} h^2$ times smaller than its present size. This happened about 10^4 yr after the Big Bang, as indicated in (10.64). Since the temperature at that time was 2.735 K multiplied by this redshift factor, the Universe was **still too hot for the formation of atoms**.

We know that matter and radiation were in equilibrium in the early Universe. We now ask the question how long this coupling between matter and radiation continued.

Photons interact with electrons through Thomson scattering. As long as electrons are free, we expect Thomson scattering to keep matter and radiation in equilibrium. **Radiation gets decoupled from matter when atoms form and all electrons get locked up inside atoms.**

The formation of atoms

We can apply the Saha [equation](#) to estimate the ionization fraction which gives a measure of the number of free electrons.

The ionization potential for hydrogen is $\chi = 13.6 \text{ eV}$, corresponding to a temperature of $1.5 \times 10^5 \text{ K}$ by (10.68). However, a simple application of the Saha [equation](#) shows that the number of free electrons becomes insignificant only when the temperature falls to a much lower value of about **3000K**. We thus conclude that the Universe becomes transparent to photons when the temperature falls below 3000 K, causing radiation to get decoupled from matter.

Interestingly, the plot of stellar opacity in Figure 2.8 shows that stellar material also becomes transparent when the temperature falls to about this value. Since the present CMBR temperature is 2.735 K, a simple application of (10.49) suggests that the Universe must have been about 1000 times smaller in size when the temperature was 3000 K. A more careful calculation gives the redshift $z_{\text{dec}} \approx 1100$ as the era when matter-radiation decoupling took place.

The Universe became transparent after this decoupling and photons no longer interacted with matter.

The formation of atoms

All the **CMBR photons** which reach us today last interacted with matter at the era of redshift $z_{\text{dec}} \approx 1100$. These photons **started as blackbody radiation of temperature 3000 K**. The redshift of 1100 has made them the **present blackbody radiation of temperature 2.735 K**.

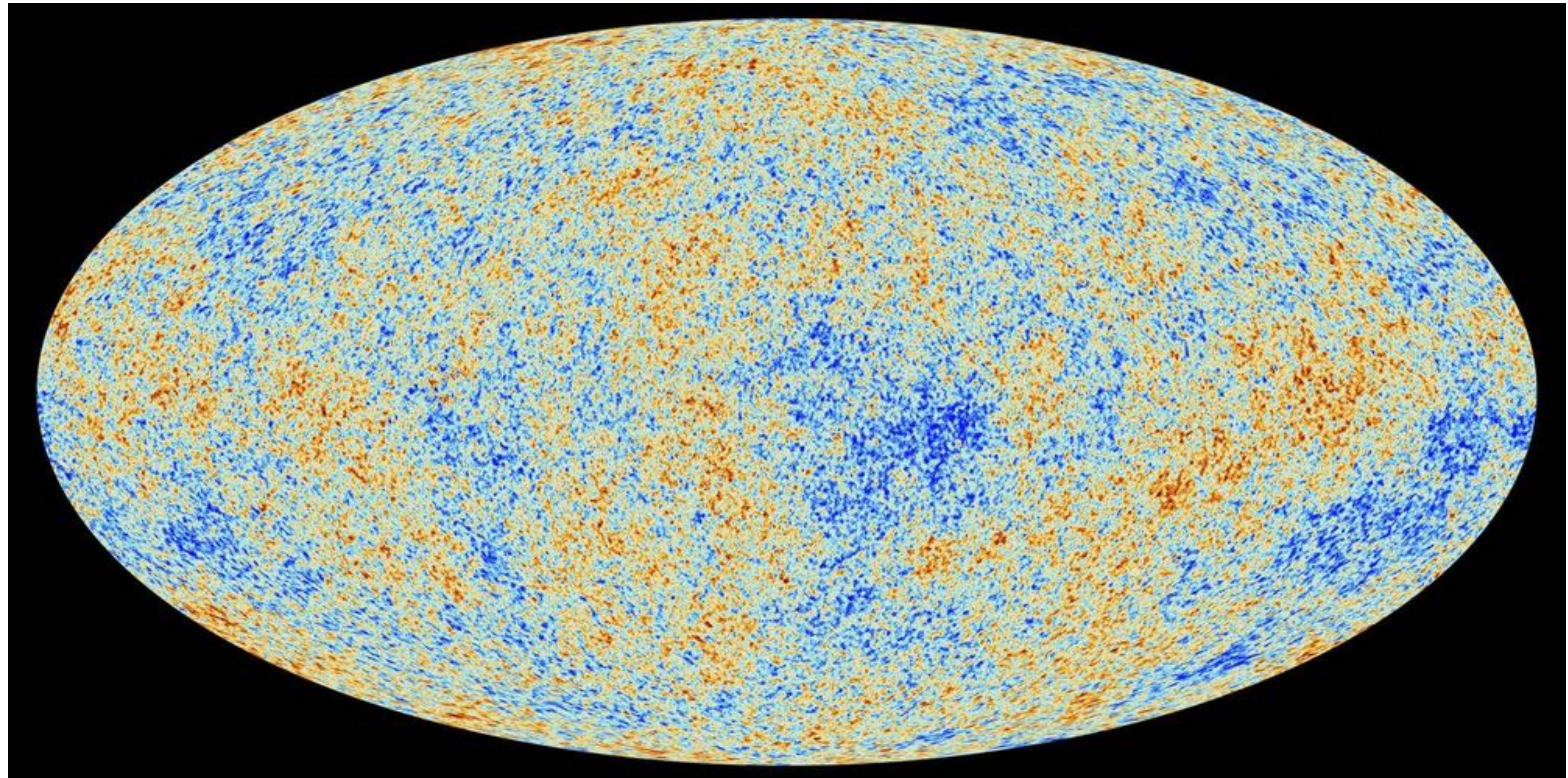
When we look at the **Sun**, we basically see **photons which last interacted with matter at the solar surface**, since the space between the solar surface and us is transparent to visible light. So the photons coming from the Sun show us the solar surface.

In exactly the same way, **the CMBR photons** coming from all directions show us a surface of primordial matter surrounding us as it existed at redshift $z_{\text{dec}} \approx 1100$. This is called the ***last scattering surface***.

If the primordial matter at redshift $z_{\text{dec}} \approx 1100$ was completely homogeneous, then this last scattering surface would appear smooth and CMBR coming from it would be totally isotropic. On the other hand, **if there were inhomogeneities in the last scattering surface, they would manifest themselves as angular anisotropies in the CMBR**.

Can we see inhomogeneities in the CMBR?

The formation of atoms



CMB measurement from the Planck satellite

Primary anisotropies in the CMBR

We believe that **the matter distribution in the primordial Universe was reasonably homogeneous**. A standard paradigm in cosmology is that there were some **small initial perturbations in matter density which kept on being enhanced with time as the Universe expanded** and eventually led to the formation of **structures that we see today** – stars, galaxies and galaxy clusters.

If this paradigm is correct, then there must have been some **density perturbations in the last scattering surface**, causing anisotropies in the CMBR. The mission COBE showed the spectrum of CMBR to be a perfect blackbody spectrum. COBE also kept looking for anisotropies in CMBR and finally discovered them. It was found that **CMBR looks exactly like blackbody radiation in all directions, but the temperature of the blackbody radiation was found to vary slightly from direction to direction**. The temperature variation was discovered to be of order

$$\frac{\Delta T}{T} \approx 10^{-5}. \quad (11.34)$$

Primary anisotropies in the CMBR

The upper panel of Figure 11.3 shows a map of this temperature anisotropy as discovered by COBE. Since COBE had an angular resolution of about 7° , the temperature variation at smaller angular scales could not be determined by COBE.

This was finally achieved by the later mission WMAP (Wilkinson Microwave Anisotropy Probe). See the lower panel of Figure 11.3.

The typical angular size of anisotropies can be used to put important constraints on various cosmological parameters.

The anisotropies in CMBR resulting from irregularities in the last scattering surface are often called ***primary anisotropies***, to distinguish them from anisotropies which may arise during the passage of the CMBR photons from the last scattering surface to us.

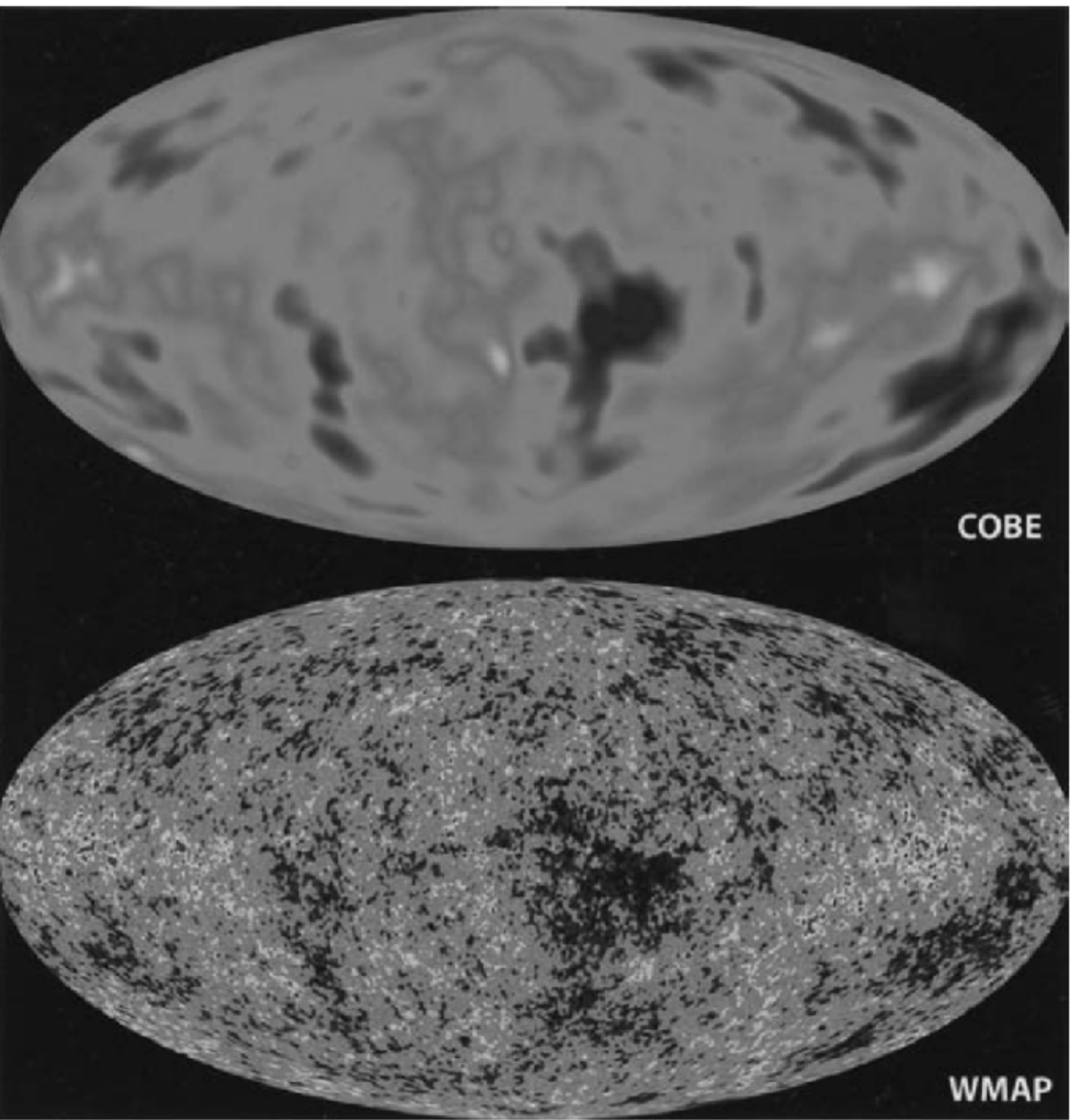
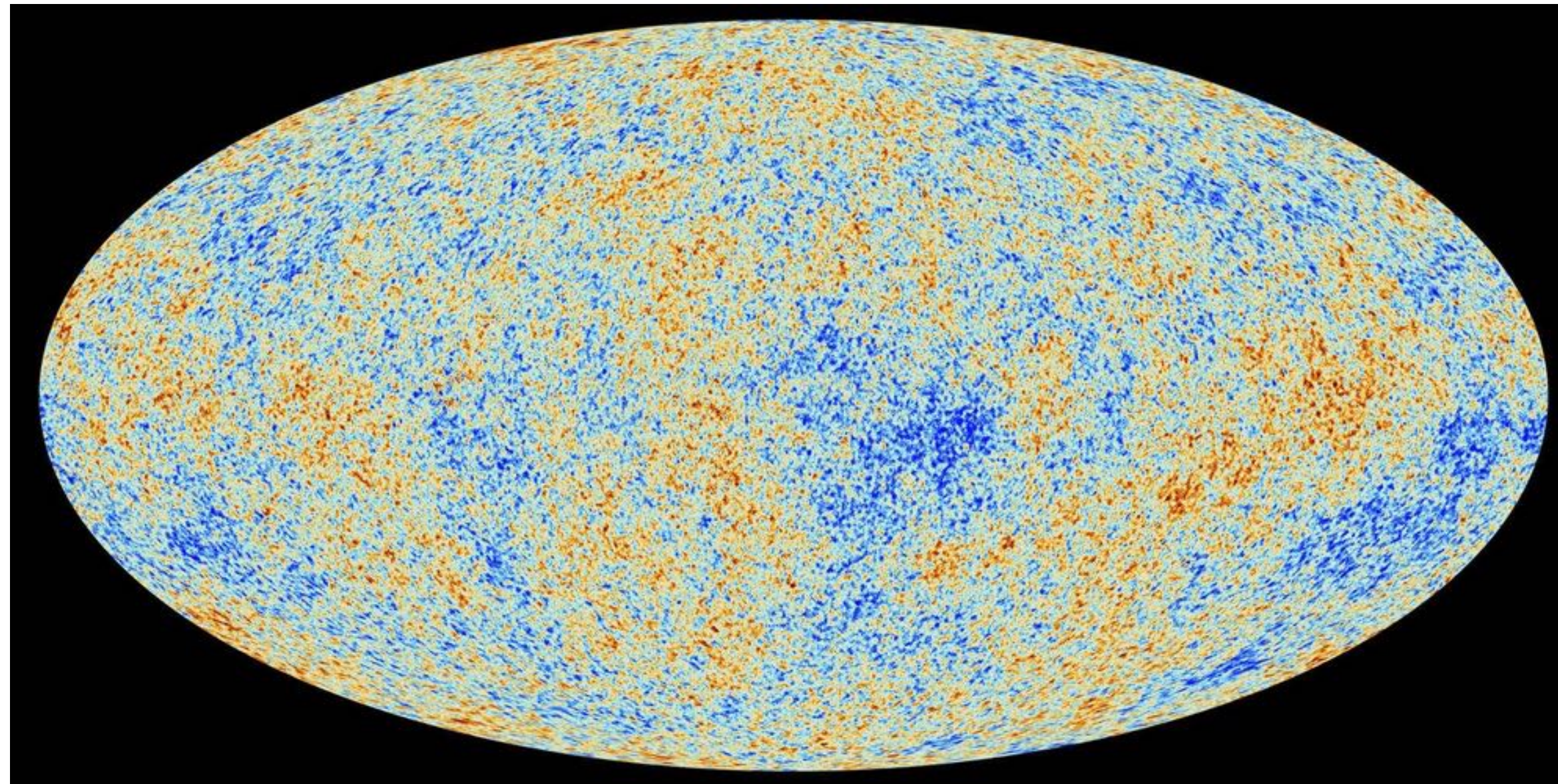


Fig. 11.3 Map of the CMBR temperature distribution in different directions of the sky, as obtained by (a) COBE ([Smoot *et al.*, 1992](#)): upper panel; and (b) WMAP ([Bennett *et al.*, 2003](#)): lower panel.

Primary anisotropies in the CMBR



CMB measurement from the Planck satellite.
This is the newest and so far most accurate
measurement.

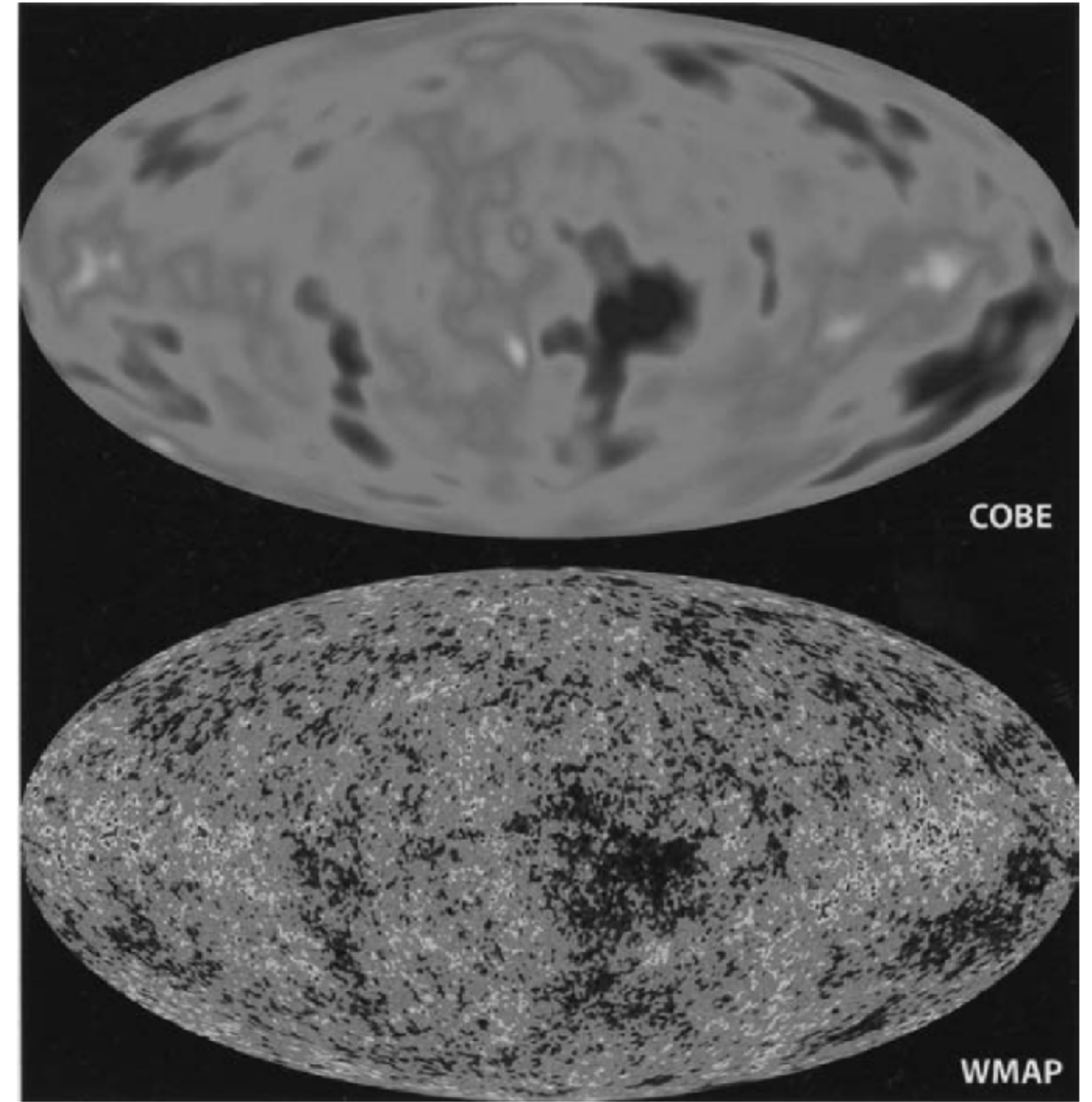


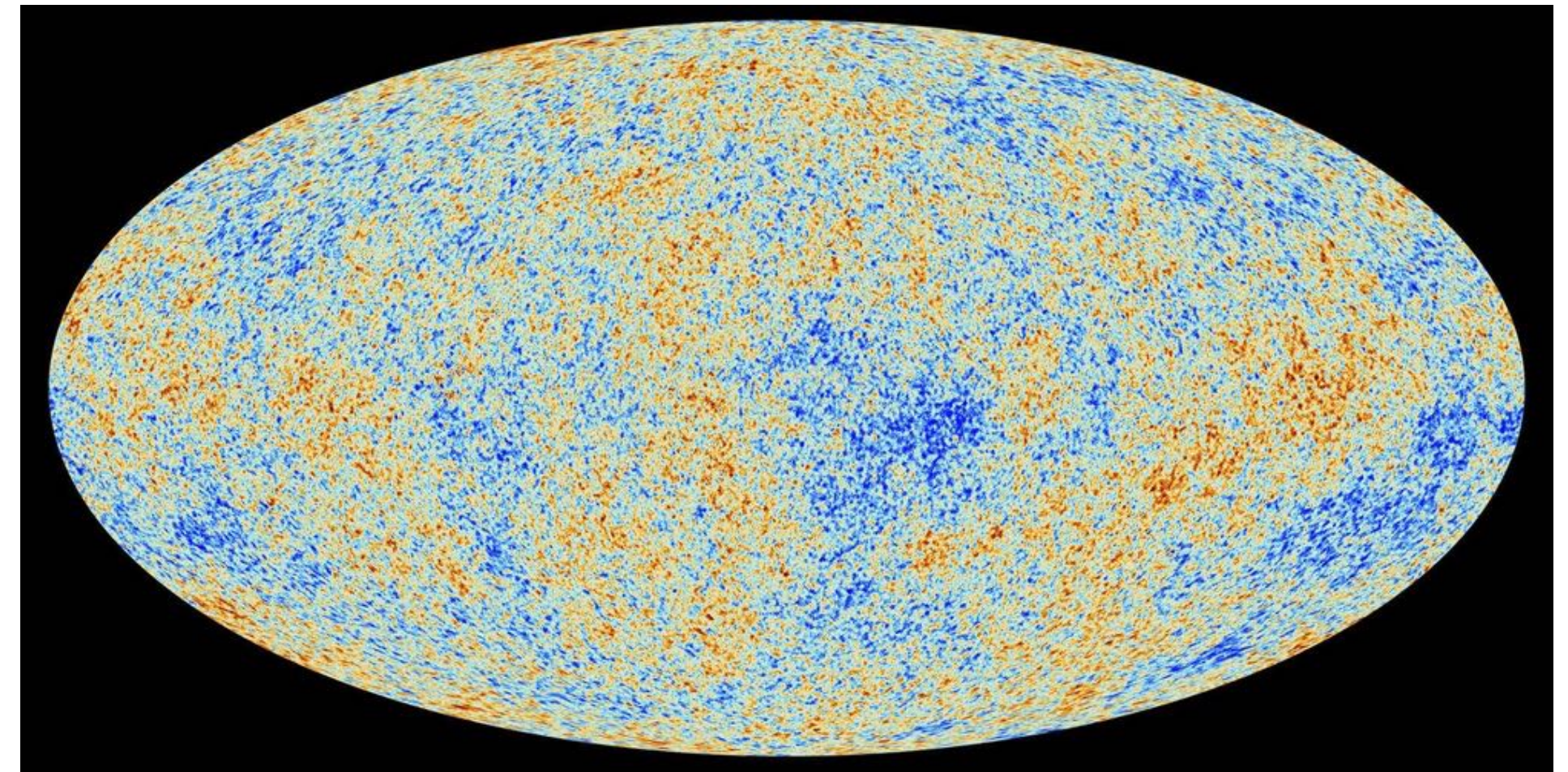
Fig. 11.3 Map of the CMBR temperature distribution in different directions of the sky, as obtained by (a) COBE ([Smoot *et al.*, 1992](#)): upper panel; and (b) WMAP ([Bennett *et al.*, 2003](#)): lower panel.

Primary anisotropies in the CMBR

The cosmic microwave background radiation is an emission of uniform, black body thermal energy coming from all parts of the sky. The radiation is isotropic to roughly one part in 100,000: the **rms variations are only $18 \mu\text{K}$** , after subtracting out a **dipole anisotropy** from the Doppler shift of the background radiation.

The latter is caused by the **peculiar velocity of the Sun relative to the comoving cosmic rest frame** as it moves at $369.82 \pm 0.11 \text{ km/s}$ towards the constellation Leo (galactic longitude 264.021 ± 0.011 , galactic latitude 48.253 ± 0.005).

The CMB dipole and aberration at **higher multipoles** have been measured, consistent with **galactic motion**.



The Sunyaev-Zeldovich effect

We have said that the **photons from the last scattering surface** reach us without interacting with matter any more. This is an almost correct statement, since most of the space between the last scattering surface and us is devoid of free electrons.

There is, however, one important exception. **Galaxy clusters contain hot gas, which is ionized and has free electrons.** So CMBR photons passing through galaxy clusters can interact with the free electrons in the hot gas.

In normal Thomson scattering, **photons scatter off electrons** without any significant change in energy. Thomson scattering involving an **energy exchange between photons and electrons** is called the **Compton effect or Compton scattering.**

While the mathematical theory of Thomson scattering can be developed by treating the photons as making up a classical electromagnetic wave, the theory of the Compton effect requires a treatment of photons as particles. **The Compton effect becomes important when the photon energy is not negligible compared to the rest mass energy of the electron** (as in the case of X-ray photons) and some energy can be transferred from the photon to the electron.

The Sunyaev-Zeldovich effect

On the other hand, **when an electron with high kinetic energy interacts with a low-energy photon, we can have the *inverse Compton effect*** in which energy is transferred from the electron to the photon. This happens when CMBR photons interact with the free electrons in a galaxy cluster, which are highly energetic because of the high temperature of the cluster gas. **This transfer of energy from the electrons in the hot cluster gas to the CMBR photons is known as the *Sunyaev–Zeldovich effect*.**

As a result of this, **some of the radio photons in the CMBR get scattered to become X-ray photons, leading to a depletion of CMBR intensity in radio frequencies in the directions of galaxy clusters.**

From this depletion in intensity, one can **estimate the optical depth (usually $\ll 1$) of CMBR photons through the cluster gas.**

For a spherical cluster of radius R_c and internal electron density n_e , the **maximum optical depth at the centre would be of order $2\sigma_T n_e R_c$** , where σ_T is the Thomson scattering cross-section.

One important **application** of the Sunyaev–Zeldovich effect is that it **can be used to estimate the distances of galaxy clusters**, thereby leading to a determination of the **Hubble constant**.

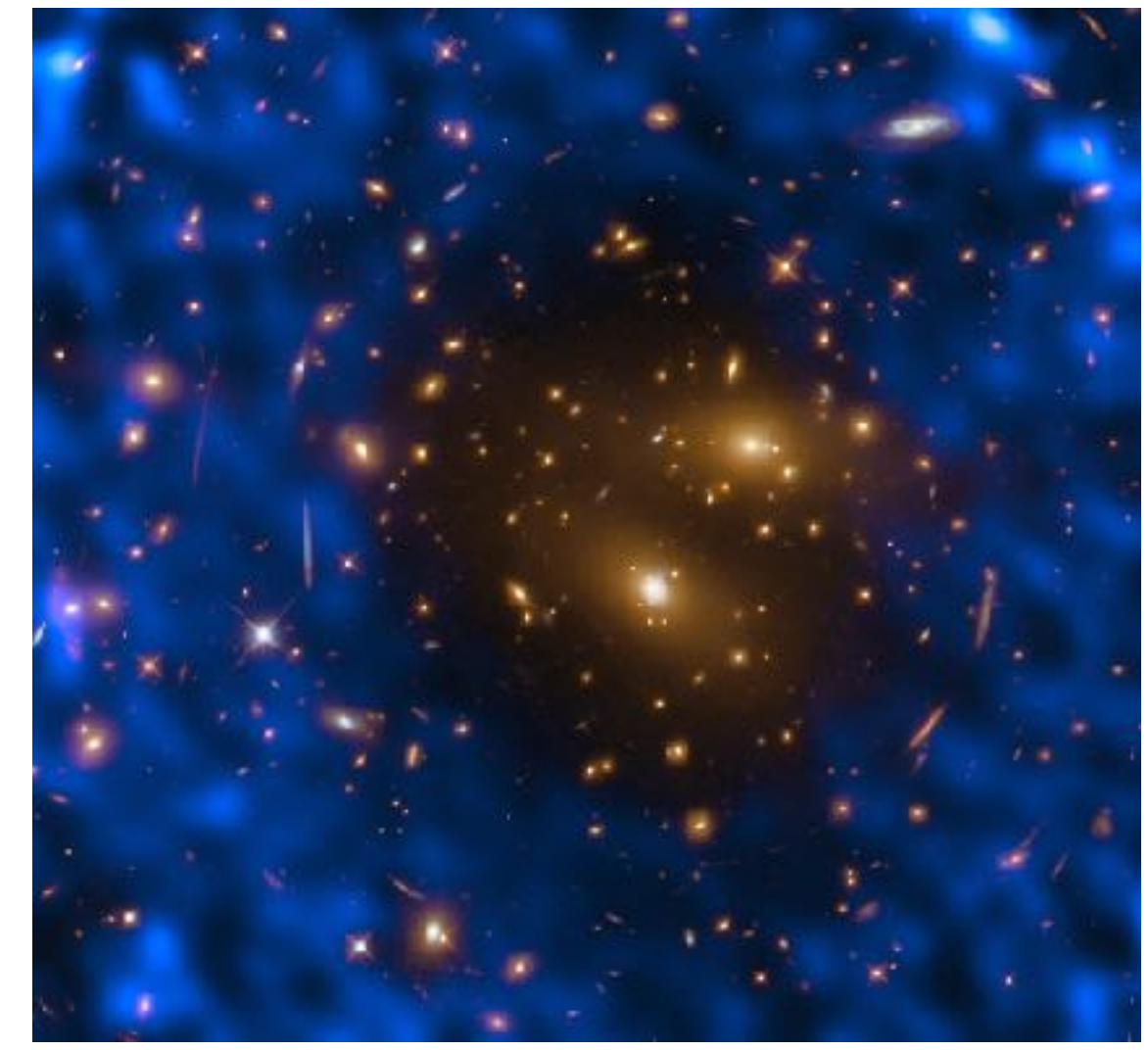
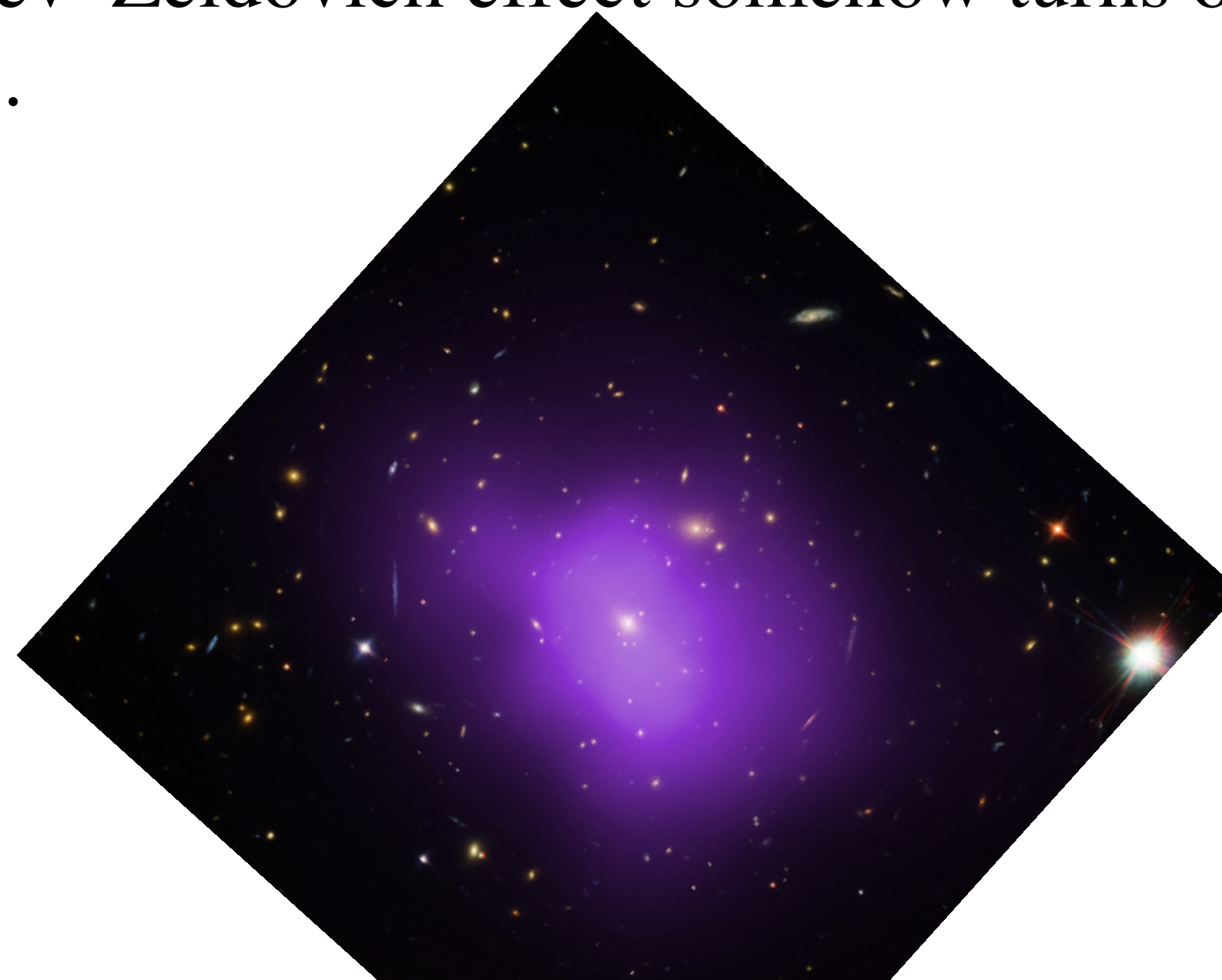
The Sunyaev-Zeldovich effect

We get $n_e R_c$ from the depletion in the CMBR intensity.

The angular size of the cluster is equal to $2R_c$ divided by its distance.

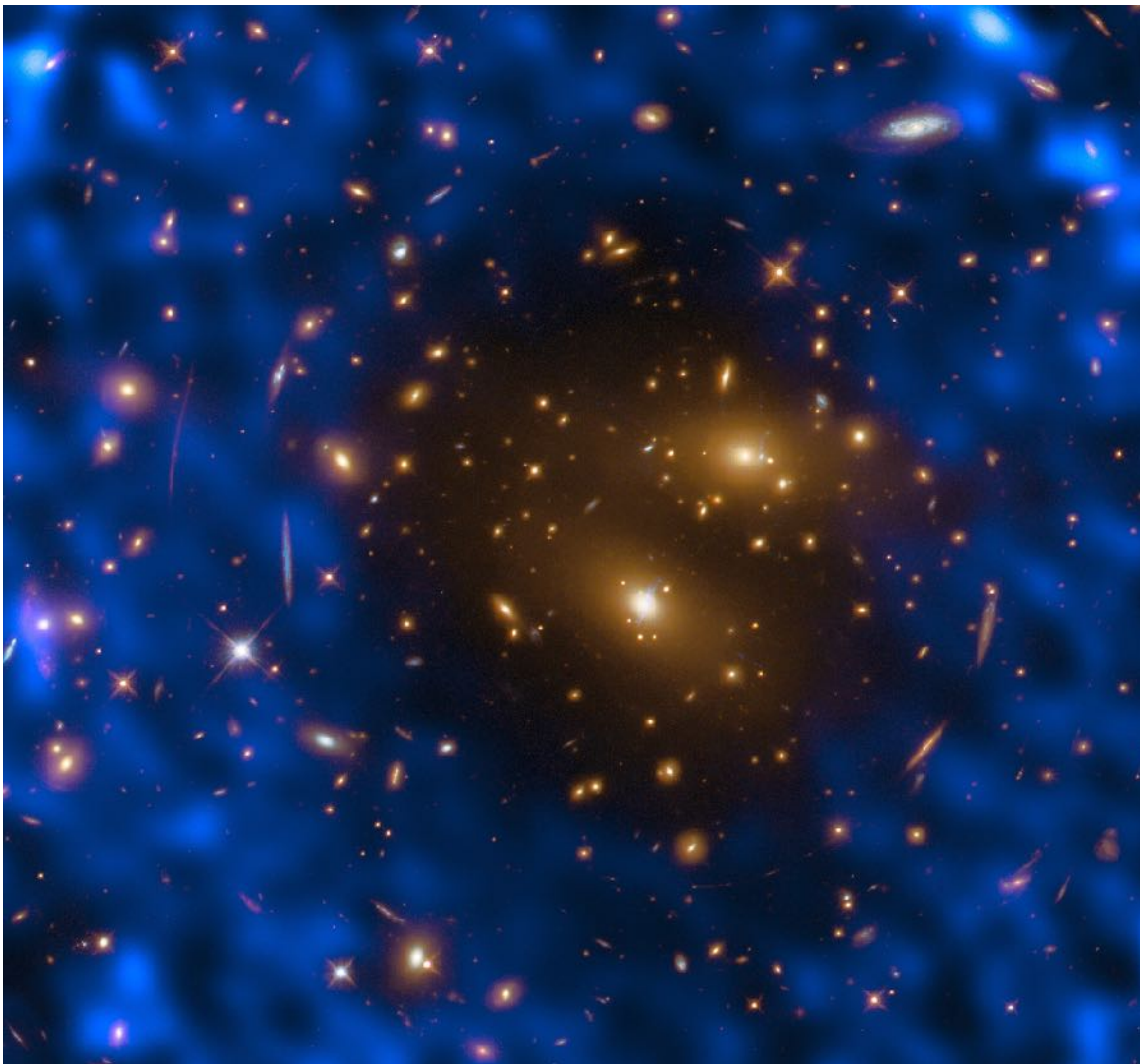
The X-ray emission from the cluster gas by bremsstrahlung is governed by (8.70), which gives the emissivity per unit volume. **On measuring the X-ray flux from the cluster received by us and combining it with the other measured quantities such as the angular size of the cluster and the depletion in the CMBR intensity, we can find the distance to the cluster.**

The Hubble constant derived from the Sunyaev–Zeldovich effect somehow turns out to be slightly lower than its value measured by the other methods.



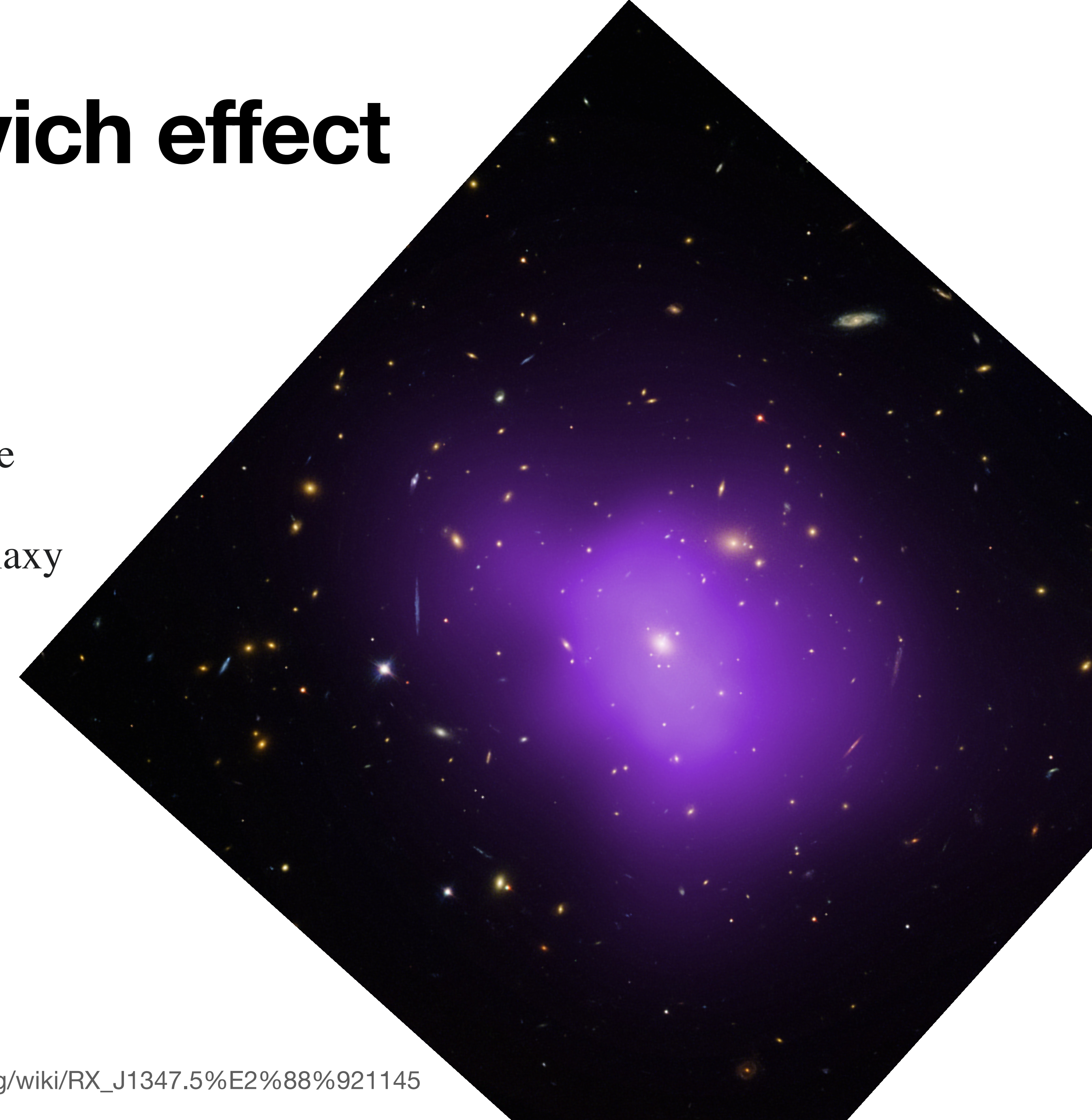
The Sunyaev-Zeldovich effect

This image shows the first measurements of the thermal Sunyaev-Zeldovich effect from the Atacama Large Millimeter/submillimeter Array (ALMA) in Chile (in blue). The target was **one of the most massive known galaxy clusters**, RX J1347.5–1145, the centre of which **shows up here in the dark “hole” in the ALMA observations**. The energy distribution of the CMB photons shifts and **appears as a temperature decrease at the wavelength observed by ALMA**, hence a dark patch is observed in this image at the location of the cluster.



The Sunyaev-Zeldovich effect

The same galaxy cluster RX J1347.5–1145, here the purple ice shows X-ray emission from the cluster. X-ray emission shows the hot ionised gas in the galaxy cluster.



Redshift $z \sim 1 - 6$

We can get direct information about some material object in the astronomical Universe if it either emits radiation or absorbs radiation passing through it. We can study the distribution of primordial matter at the moment of its decoupling from radiation by analysing the **CMBR which was emitted by this matter**. **After the matter-radiation decoupling, however, the matter in the Universe became transparent and did not emit any more radiation until stars and galaxies formed long afterwards.** The era between the matter-radiation decoupling (around $z \sim 1100$) and the era when the first stars formed is **often called the ‘dark age’ in cosmology**.

During this dark age, **matter did not emit any radiation** that we can detect today, although the CMBR that had got decoupled from matter remained present and kept on being redshifted to lower temperatures as the Universe expanded. We now discuss observations which give us an indication how the Universe might have looked like at the end of the dark age, when there were again radiation-emitting sources which we can try to discover today.

Redshift $z \sim 1 - 6$

This new field of studying astronomical objects at **redshifts lying in the range $z \sim 1-6$** has blossomed only in the last few years when telescopes like the Hubble Space Telescope (HST) and now the James Webb Space Telescope (JWST) allowed astronomers to study faraway faint sources which could not be studied earlier.

We shall restrict our discussion here only to the question of what the Universe looked like at these high redshifts – especially to the question whether the Universe looked substantially different from the present Universe and whether **we see clear indications of evolution**.

Another important issue is whether we can determine important cosmological parameters (such as $\Omega_{M,0}$) by using high-redshift observations. Since this topic requires a knowledge of relativistic cosmology, we postpone the discussion of this important topic to [Chapter 14](#).

**What is the highest redshift object currently known?
Is it a quasar?**

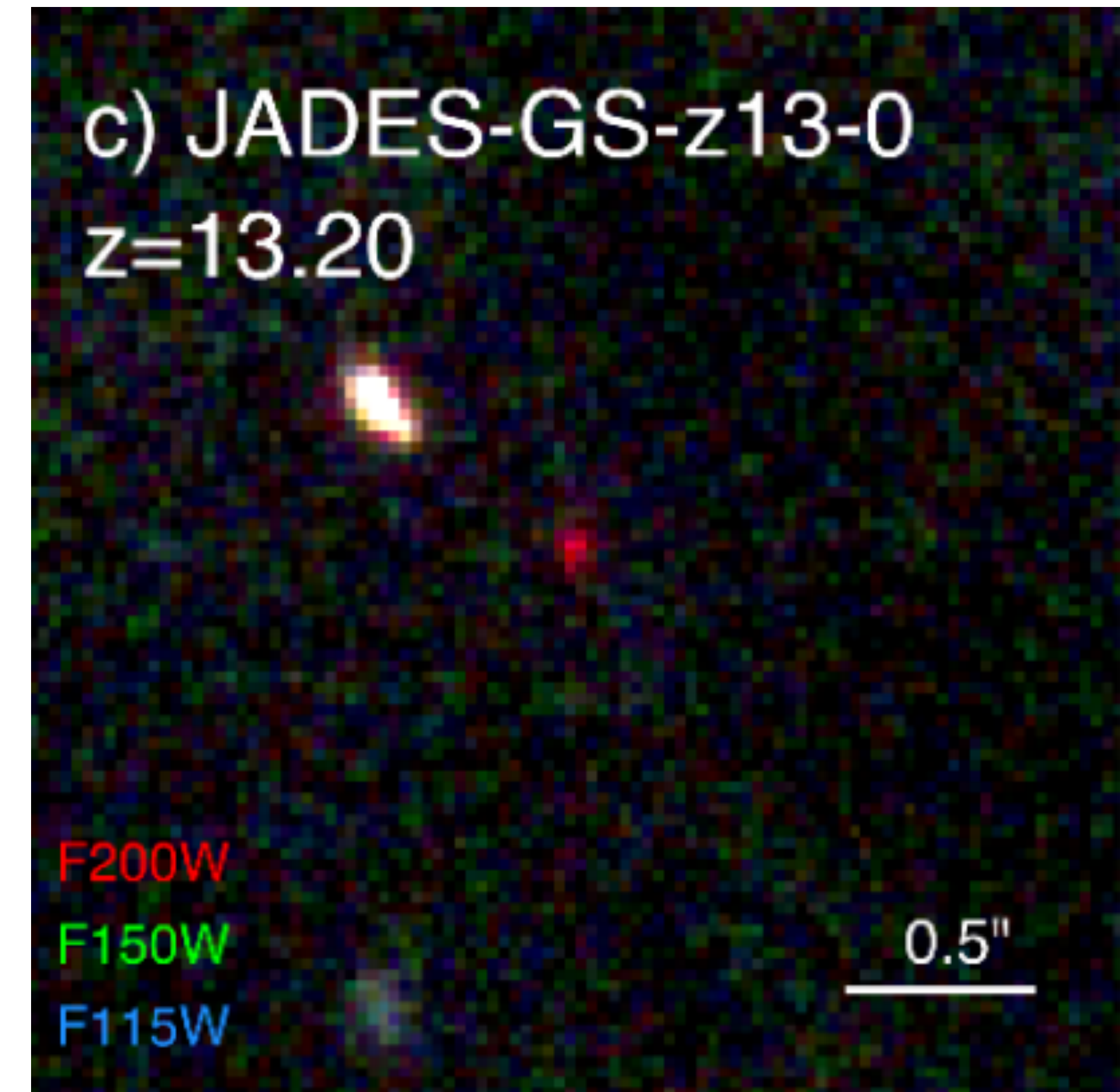
Quasars

This object was detected with the James Webb telescope and has an approximate redshift of $z = 13.20$ (redshift is determined with spectroscopy). The **age of the Universe is estimated to be $z = 13.787$**

Identified as a Lyman-break galaxy. **Lyman-break galaxies are star-forming galaxies at high redshift** that are selected using the differing appearance of the galaxy in several **imaging filters** due to the position of the Lyman limit.

Radiation at higher energies than the Lyman limit at 912 Å is almost completely absorbed by neutral gas around star-forming regions of galaxies. In the rest frame of the emitting galaxy, the emitted spectrum is bright at wavelengths longer than 912 Å, but very dim or imperceptible at shorter wavelengths—this is known as a "dropout", or "break", and can be used to find the position of the Lyman limit. At high redshift galaxies this break is shifted to optical or infrared wavelengths.

The most distant object in the Universe? In 2023.



Quasars

The **highest-redshift quasar known** (as of December 2017) was ULAS J1342+0928, with a **redshift of 7.54**, which corresponds to a comoving distance of approximately 29.36 billion light-years from Earth.

Artist impression of a quasar



Quasars and galaxies at high redshift

Since **quasars are intrinsically brighter than normal galaxies**, they are much more likely to be discovered at large redshifts compared to normal galaxies. Quasars were therefore amongst the **first objects at high redshifts to be studied systematically** by astronomers.

Figure 11.4 shows a plot of quasar number density in co-moving volume as a function of redshift.

Keeping in mind that **higher redshifts mean earlier times**, it is very clear from this plot that the quasar number density has changed with the age of the Universe. It was **highest around redshift $z \sim 2$** .

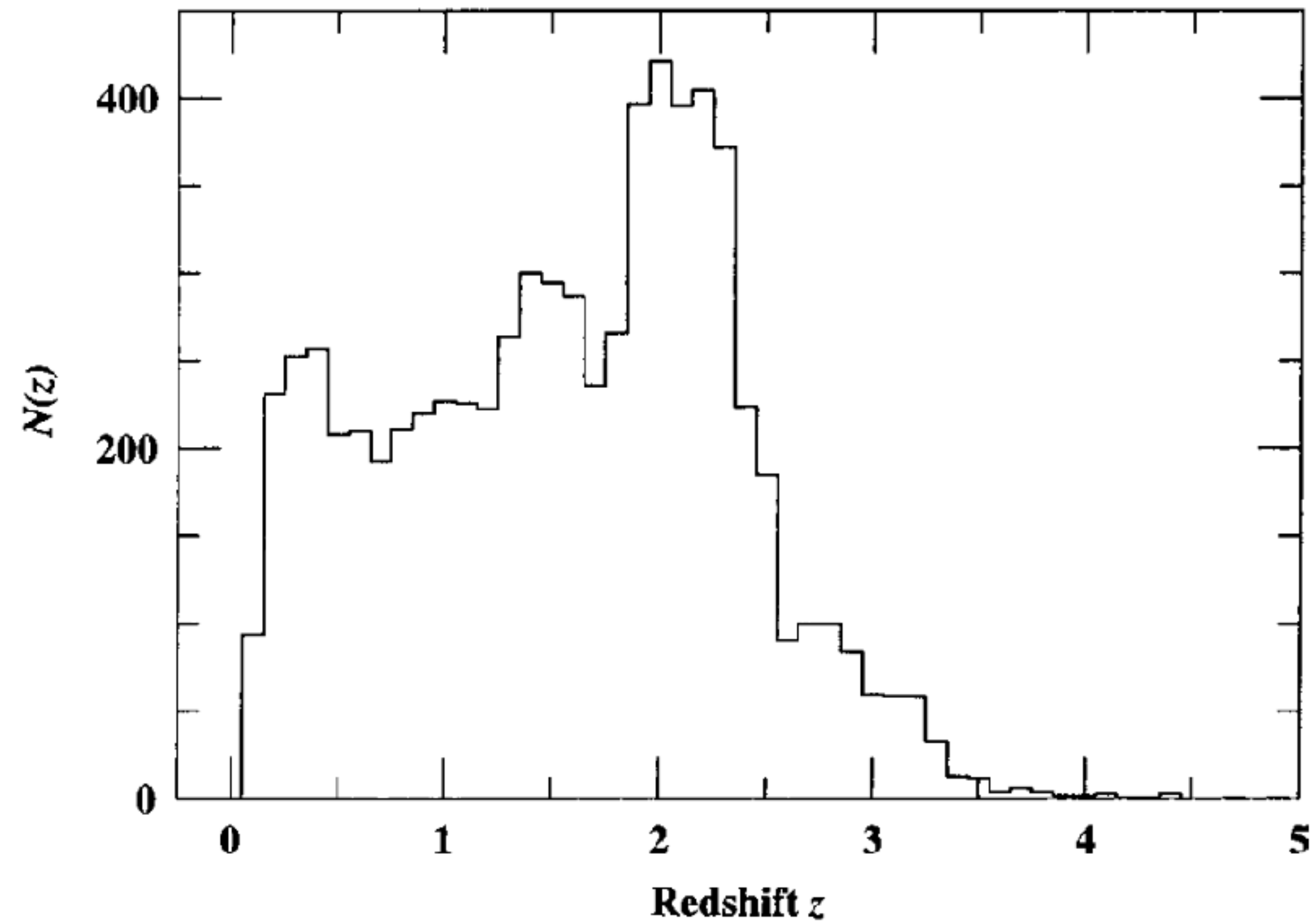


Fig. 11.4 The plot of quasar number density in co-moving volume as a function of redshift. From Peterson (1997, p. 17), based on the data catalogued by Hewitt and Burbidge (1993). (©Cambridge University Press.)

Quasars and galaxies at high redshift

The evolution of quasar number density was one of the first pieces of evidence of evolution in the world of galaxies discovered by astronomers.

Quasar energy emission is caused by gas falling into a **supermassive black hole**.

After the formation of a galaxy, it presumably takes **some time for a supermassive black hole to develop at its centre**. It is likely that **the majority of galaxies formed well before the redshift of $z \sim 2$ when quasars were most abundant**, but central black holes took time to form. Since the black hole has to be fed with infalling gas in order to produce quasar activity, we expect such activity to be **more prevalent when more gas is available**.

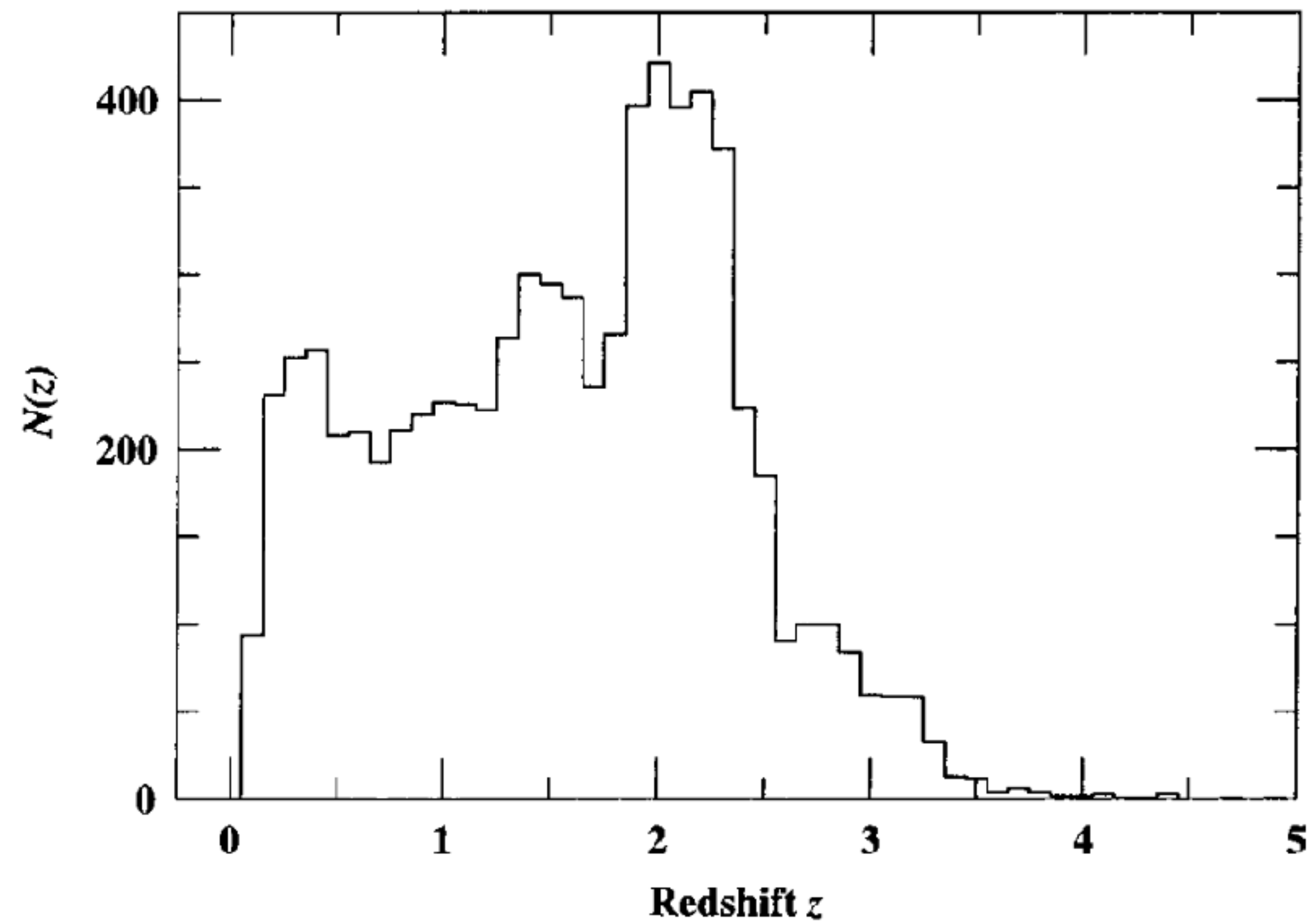


Fig. 11.4 The plot of quasar number density in co-moving volume as a function of redshift. From Peterson (1997, p. 17), based on the data catalogued by Hewitt and Burbidge (1993). (©Cambridge University Press.)

Quasars and galaxies at high redshift

It is possible that the **availability of gas decreases with the age of a galaxy** as more gas is used up for star formation.

This scenario gives a qualitative explanation of why the quasar number density was maximum around $z \sim 2$. **At earlier times, not many galaxies had supermassive black holes** at their centres. **At later times, the availability of gas for feeding the black holes decreased.**

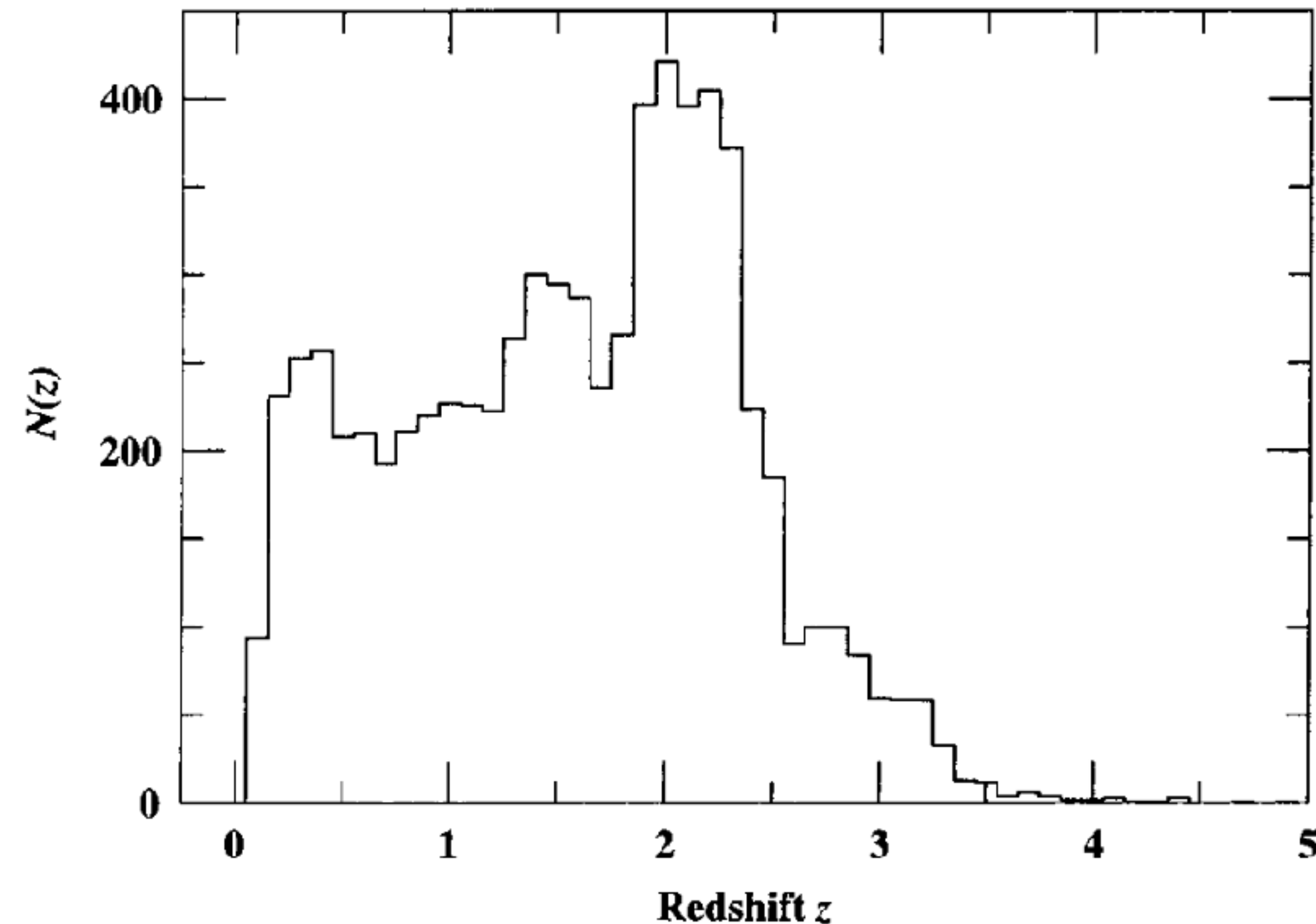


Fig. 11.4 The plot of quasar number density in co-moving volume as a function of redshift. From Peterson (1997, p. 17), based on the data catalogued by Hewitt and Burbidge (1993). (©Cambridge University Press.)

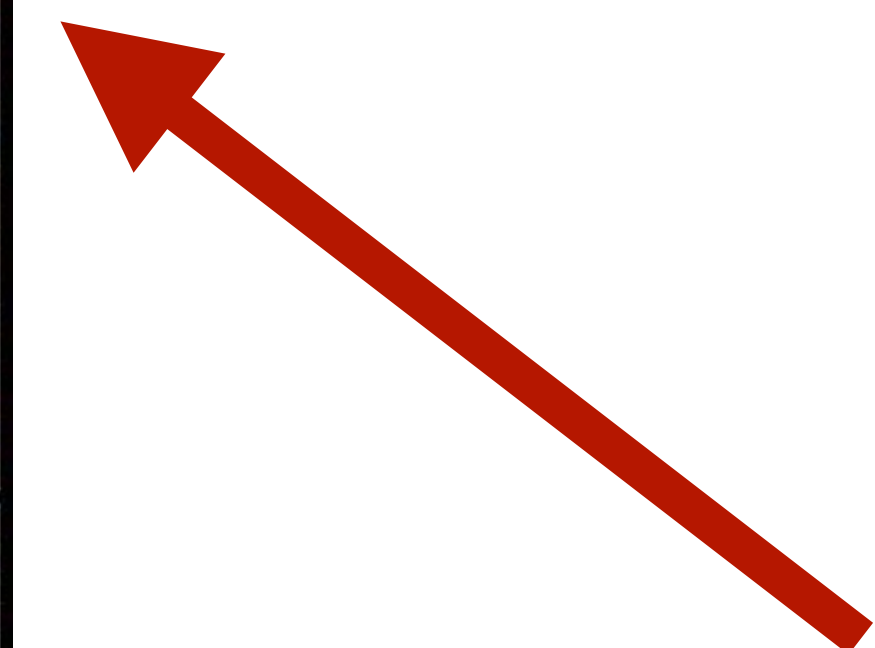
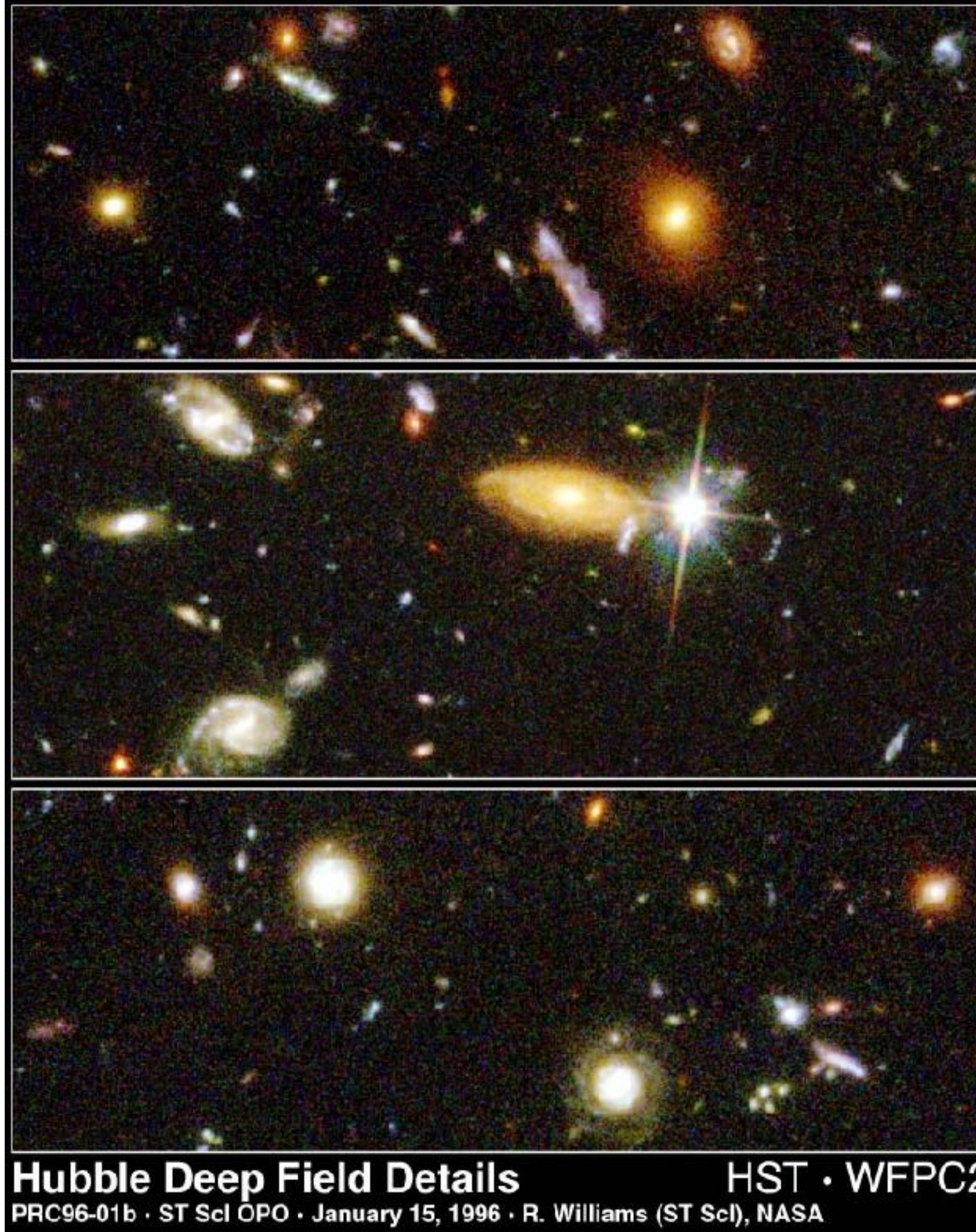
Quasars and galaxies at high redshift

Since a powerful telescope can detect many millions of galaxies, it is notoriously difficult to isolate high-redshift galaxies in this vast sample. Also, a high-redshift normal galaxy would appear very faint to us and can be imaged only after a very long exposure.

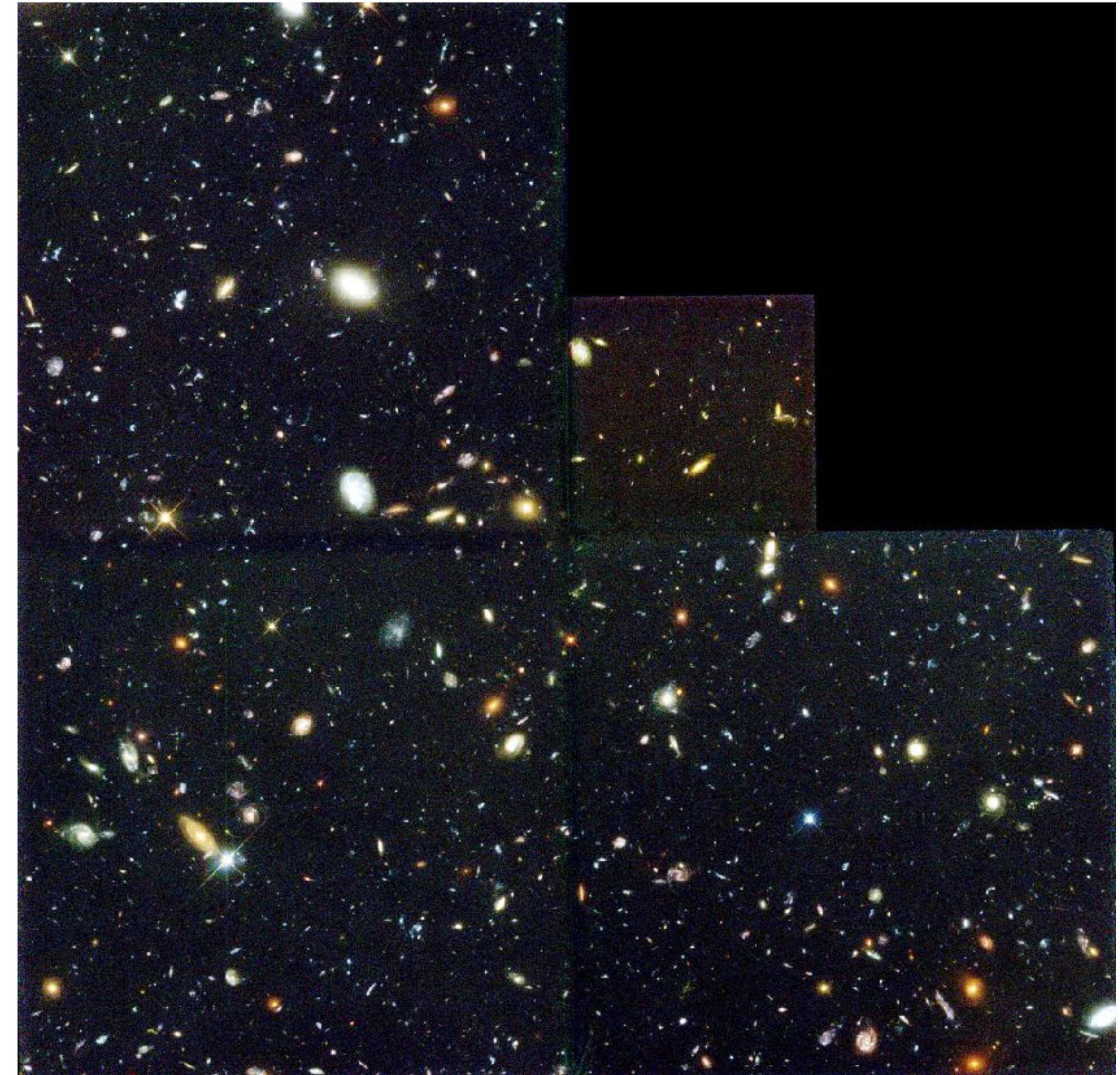
In December 1995 HST imaged a very small portion of the sky without any special characteristics for about 10 days. The resulting image, known as the *Hubble Deep Field*, is shown in [Figure 11.5](#). It shows about **1500 galaxies at various stages of evolution**, some of the galaxies being much fainter than any galaxies imaged before. From a detailed analysis of the Hubble Deep Field, it is concluded that **the star formation rate was maximum during redshifts $z \sim 1\text{--}1.5$.**

To sum up, although some galaxies and quasars might have formed even before $z \sim 6$, such phenomena as quasar activity and star formation reached their maxima much later. It is, however, clear that the Universe revealed by the furthest quasars and furthest normal galaxies is quite different from the present Universe. There is unmistakable evidence for evolution. We now consider the material in the space between galaxies, to find out if this material gives any more clues in completing the story of the earliest galaxies.

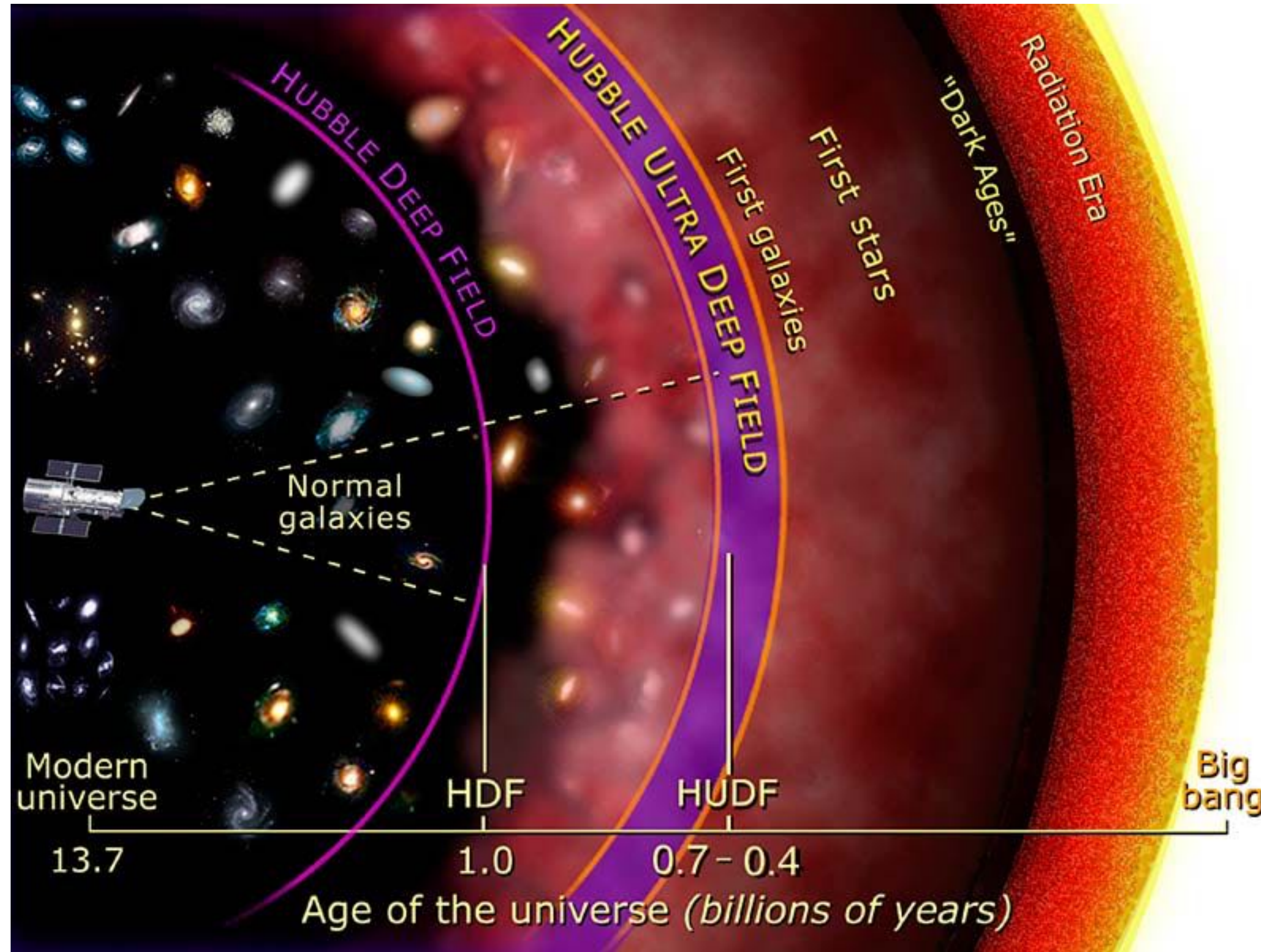
Quasars and galaxies at high redshift



The Hubble Deep Field



Quasars and galaxies at high redshift



Quasars and galaxies at high redshift



the James Webb Space Telescope spent over 20 hours observing the long-studied Ultra Deep Field of the NASA/ESA Hubble Space Telescope

The intergalactic medium

Apart from the gas in clusters of galaxies, **is there matter in regions of space between clusters and outside of galaxies?**

Even if there is matter in the intergalactic space, the question is how we can detect it. **The emission from the intergalactic medium lying outside galaxy clusters has not been detected** in any band of the electromagnetic spectrum.

The only other way of checking the existence of the intergalactic medium is to **look for absorption lines in the spectra of objects lying very faraway**. Since quasars are the most faraway objects which are bright enough to obtain spectra from, looking for **absorption lines in the spectra of quasars** is the best way of searching for the intergalactic medium.

Let us consider the **Lyman- α absorption line** caused by the **transition $1s \rightarrow 2\ p$ in a hydrogen atom**. If an absorbing system is **mainly made up of neutral hydrogen atoms**, then we expect this line to be **one of the strongest absorption lines**. The rest wavelength of this line is $\lambda_{L\alpha} = 1216\text{ \AA}$.

The intergalactic medium

Suppose a quasar is at redshift z_{em} . Since quasars typically have **broad emission lines** at the redshifted wavelength $(1 + z_{\text{em}})\lambda_{\text{L}\alpha}$ of the Lyman- α line.

If there is some **absorbing material** on the line of sight lying at some **intermediate redshift** z_{abs} (obviously we expect $0 < z_{\text{abs}} < z_{\text{em}}$), then we expect absorption at wavelength $(1 + z_{\text{abs}})\lambda_{\text{L}\alpha}$. If there is neutral hydrogen gas all along the line of sight, then we would expect to see an **absorption trough** from $\lambda_{\text{L}\alpha}$ to $(1 + z_{\text{em}})\lambda_{\text{L}\alpha}$ in the spectrum of the quasar corresponding to the full run of possible values of z_{abs} .

The presence or absence of such an absorption trough in the spectrum of a distant quasar would give us an **estimate of the amount of neutral hydrogen gas over the line of sight**.

The intergalactic medium

Figure 11.6 shows the spectrum of a **quasar at redshift $z_{\text{em}} = 2.60$** , for which the **Lyman- α emission line** is at 4380 \AA .

We, however, do not see a continuous absorption trough from 1216 \AA to 4380 \AA . Instead of a trough, we find a large number of narrowly spaced absorption lines. These absorption lines are collectively referred to as the ***Lyman- α forest***.

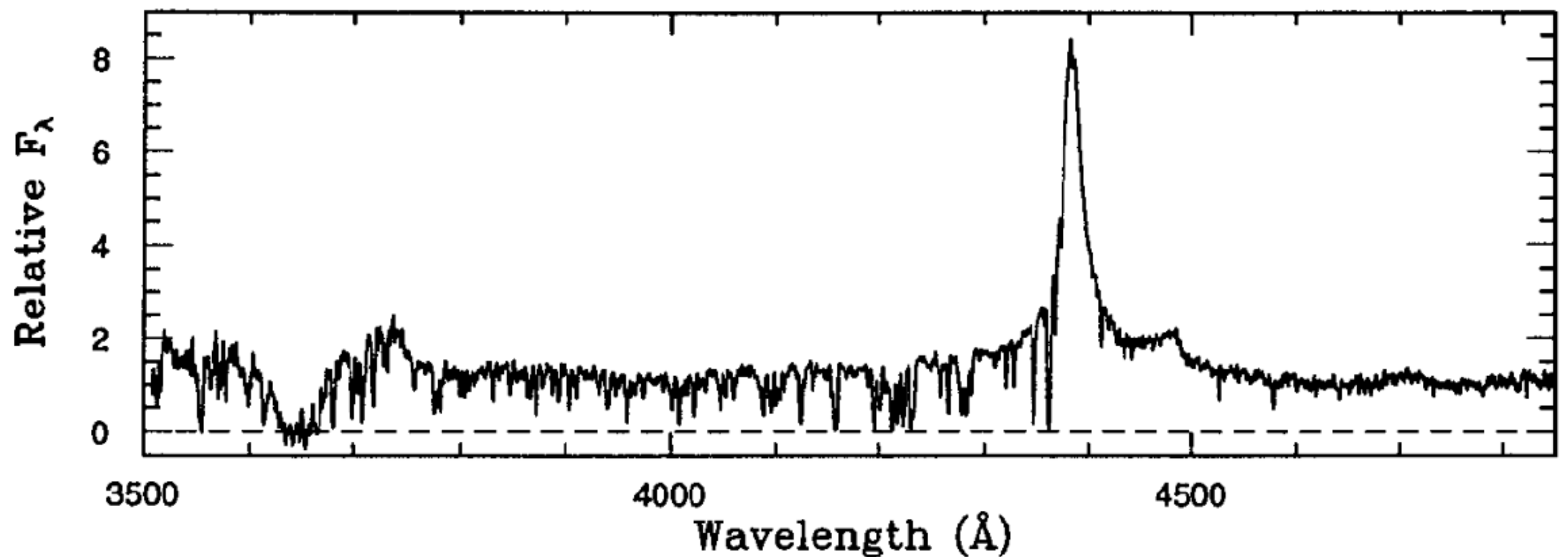


Fig. 11.6 The spectrum of a quasar at redshift $z_{\text{em}} = 2.6$. From Wolfe *et al.* (1993). (©American Astronomical Society. Reproduced with permission from *Astrophysical Journal*.)

The intergalactic medium

This implies that we **do not have a uniform distribution of neutral hydrogen gas along the line of sight**. There must be **many clouds of neutral hydrogen lying on the path at different redshifts**, which are causing the absorption lines.

In the particular spectrum shown in [Figure 11.6](#), there is a **prominent absorption feature** at 3650 \AA (corresponding to redshift $z_{\text{abs}} = 2.0$) where the radiation seems to fall almost to zero intensity. **There must be a very large cloud at this redshift $z_{\text{abs}} = 2.0$.** Such large dips in the spectra indicating the presence of large hydrogen clouds are found very often in the spectra of many distant quasars.

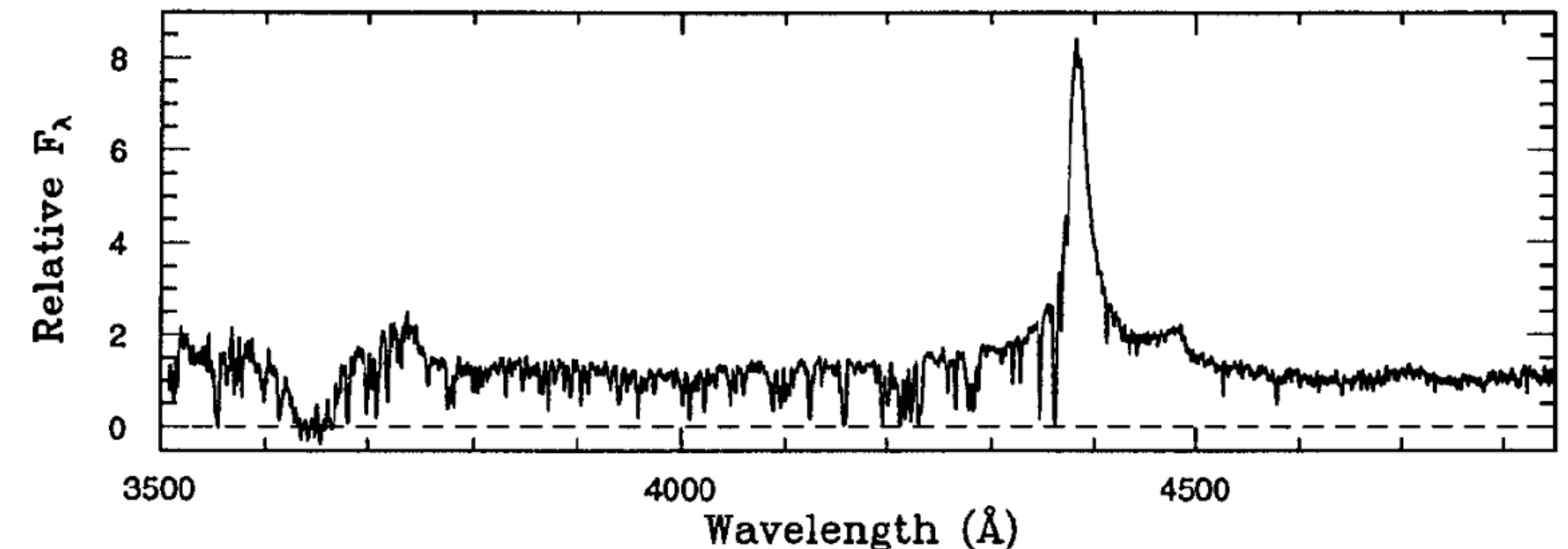


Fig. 11.6 The spectrum of a quasar at redshift $z_{\text{em}} = 2.6$. From [Wolfe et al. \(1993\)](#). (©American Astronomical Society. Reproduced with permission from *Astrophysical Journal*.)

Quasar spectra

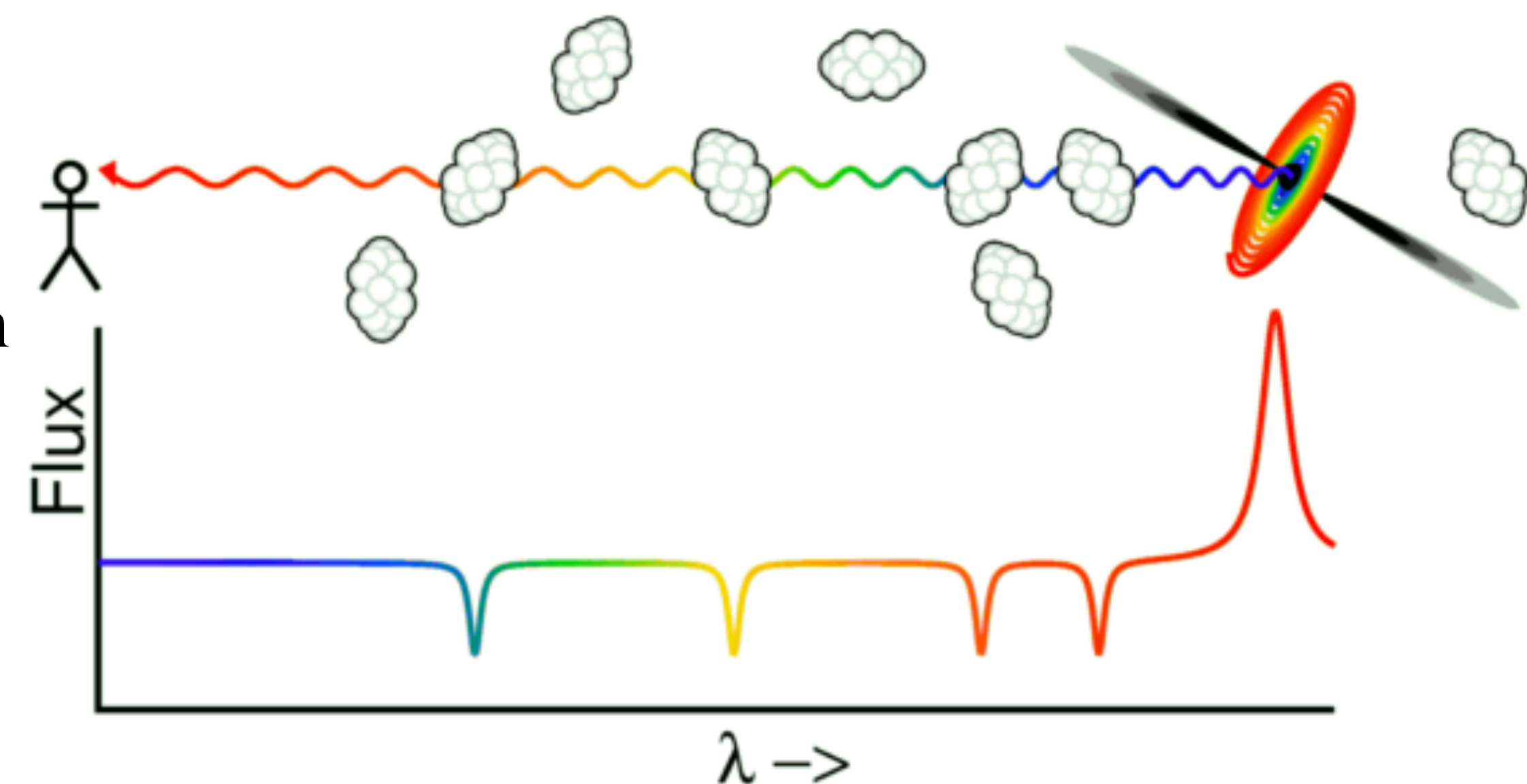
Absorption lines may also be present in some quasar spectra.

In particular, **Doppler-broadened absorption lines**, found in up to 10% of the spectra of quasars, originate from sources with **speeds exceeding 10^4 km s^{-1}** . These lines are believed to be **associated with the quasar itself**.

Many additional **narrow absorption lines** are typically seen in the spectra of quasars with high redshifts ($z > 2.2$) due to the **Lyman series of hydrogen** and metals such as **C IV and Mg II**.

These lines would normally appear at ultraviolet wavelengths but have been **redshifted into the visible spectrum** by the recessional velocity of the absorbing material.

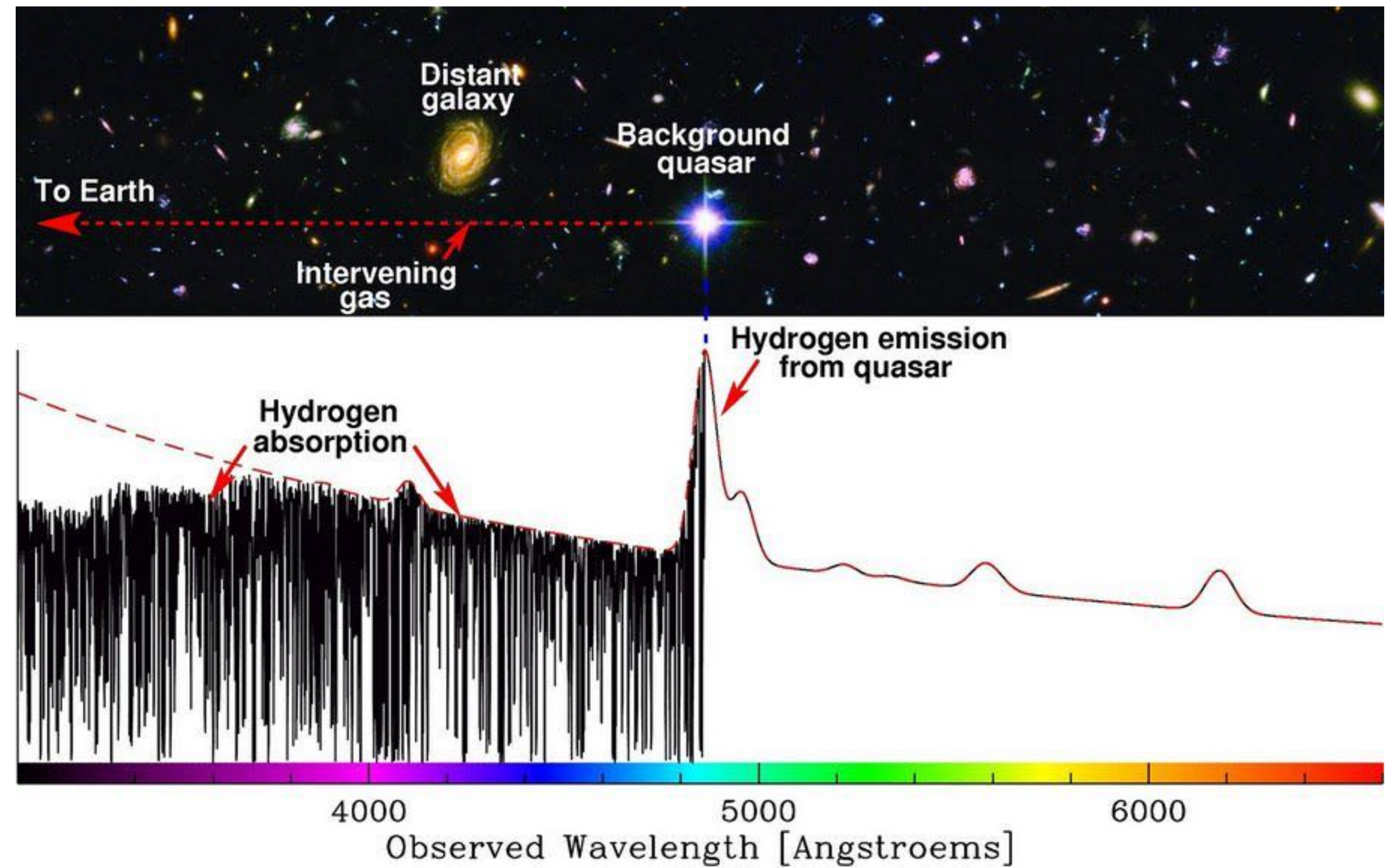
The absorption lines of a given quasar can be placed into **different groups that share common redshifts**. The various groupings of lines are thought to arise from **clouds of intervening material** that lie between the quasar and Earth.



Quasar spectra

The Lyman alpha forest:

In astronomical spectroscopy, the Lyman-alpha forest is a series of absorption lines in the spectra of distant galaxies and quasars arising from the Lyman-alpha electron transition of the neutral hydrogen atom. As the light travels through multiple gas clouds with different redshifts, multiple absorption lines are formed.



The intergalactic medium

Here we summarize the main conclusions qualitatively.

The **absence of an absorption trough**, which is often referred to as the *Gunn–Peterson test*, shows that **there is very little neutral hydrogen gas outside the clouds** and one quantitatively finds that the **number density of hydrogen atoms** has to be less than about 10^{-6} m^{-3} . For the sake of comparison, remember that the density of X-ray emitting gas in galaxy clusters is of order $10^3 \text{ particles m}^{-3}$.

The **large hydrogen clouds producing prominent dips** in the quasar spectra are estimated to have **masses comparable to the mass of a typical galaxy**. The most obvious possibility is that **these are galaxies in the making**.

The **smaller clouds producing the absorption lines** of the Lyman- α forest, however, have much smaller masses of the order of a few hundred M_\odot . Careful analysis of observational data shows that these smaller clouds are most abundant at redshifts $z \approx 2\text{--}3$ and become much less abundant at lower redshifts.

The intergalactic medium

Neutral hydrogen is mainly found inside isolated clouds. There is very little neutral hydrogen outside these clouds.

But does this mean that there is no material outside the clouds and space is really empty in those regions?

A more plausible assumption is that there is **hydrogen outside the clouds, but it has been ionized and hence is not producing the Lyman- α absorption line.**

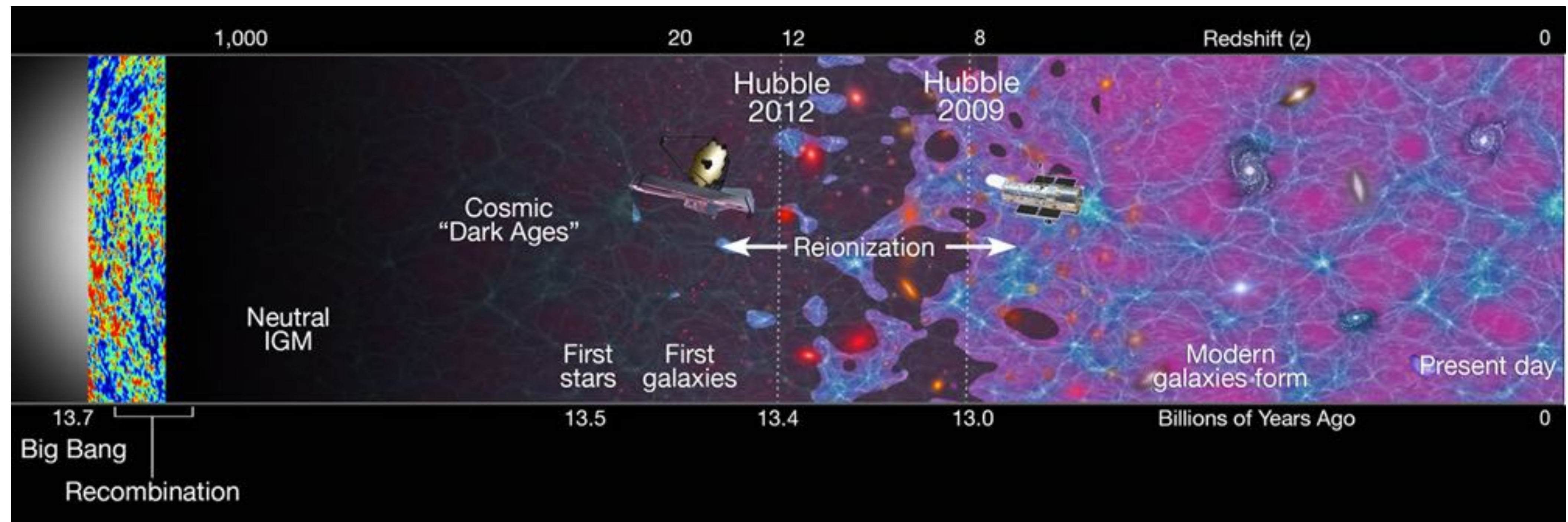
Matter was ionized before $z \approx 1100$. Then neutral atoms formed, leading to the matter-radiation decoupling. **When the first stars, galaxies and quasars started forming, the ionizing radiation from these objects presumably ionized the intergalactic medium again. This is called the *reionization*.**

The **absence of neutral hydrogen atoms** between the distant quasars and us (apart from the Lyman- α clouds) is believed to be a **consequence of this reionization**.

However, **if light started from a very distant quasar before the reionization, then the light path would initially pass through space filled with neutral hydrogen and we would expect to see a Gunn–Peterson trough in the spectrum at the lower-wavelength side of the redshifted Lyman- α line.** There are indications that **quasars with redshifts larger than $z \approx 6$ show such troughs in their spectra.**

The intergalactic medium

Altogether, we get a picture of the Universe at redshifts $z \sim 2\text{--}6$ which is very different from the present-day Universe. Already some quasars have formed and ionized the intergalactic medium. Embedded in this ionized medium, there are clouds of neutral hydrogen (presumably their interiors are shielded from ionizing photons due to higher densities) with masses of order a few hundred M_\odot . There are also more massive clouds which appear like galaxies in the making.



Structure formation

Matter was distributed fairly uniformly at the era $z \approx 1100$ when matter-radiation decoupling took place, the **density perturbations at that era being of the order of 10^{-5} .**

On the other hand, the **observations suggest that the first stars, galaxies and quasars should have formed some time before $z \approx 6$.**

How do we connect the two?

Presumably **the very small density perturbations present in era $z \approx 1100$ grew by gravitational instability to become the first stars and galaxies before $z \approx 6$.** Understanding the details of how this happened is the subject of ***structure formation***.

This is an enormously complex subject on which quite a lot of research is being done at the present time. Here we shall touch upon only some of the key issues.

Structure formation

$$k_J^2 = \frac{4\pi G\rho_0}{c_s^2}. \quad (8.21)$$

Gravitational instability → density enhancements having masses larger than the Jeans mass keep growing due to the stronger gravitational forces in the regions of density enhancements.

To understand the **growth of density perturbations in the expanding Universe**, we have to carry out the Jeans analysis against an expanding background. This analysis is somewhat more complicated. Here we shall not reproduce that derivation. Let us summarize the **main conclusions** only.

1. It is found that the **perturbations remained frozen and could not grow as long as the Universe was radiation-dominated**.
2. **Only after the Universe becomes matter-dominated, can those perturbations grow** for which the wavenumber k is less than k_J given by (8.21).
3. A growing density perturbation in the matter-dominated expanding Universe is found to **grow as**

$$\frac{\delta\rho}{\rho} \propto t^{2/3}. \quad (11.35)$$

Structure formation

According to (10.60), the scale factor a in the matter-dominated Universe also grows as the $2/3$ power of t . On the basis of (10.60) and (11.35), we can write

$$\frac{\delta\rho}{\rho} \propto a. \quad (11.36)$$

It should be remembered that this result is **based on a linear analysis**, like the linear analysis presented in §8.3. When the perturbation grows to be of the order of 1, the nonlinear effects become important and thereafter the perturbation can grow much faster than what is suggested by (11.36).

The result (11.36) at once leads us to a **difficulty**. The density perturbations were of order 10^{-5} at the era $z \approx 1100$. Since the scale factor has grown by a factor of 10^3 between that era and the present time, a straightforward application of (11.36) suggests that $\delta\rho/\rho$ at the present time should be of the order of only 10^{-2} . This certainly contradicts the existence of various structures in the Universe that we see at the present time. Since 10^{-2} is quite **small compared to 1**, we cannot hope to get around this difficulty by invoking nonlinear effects.

What is happening?

Structure formation

To find a clue for solving this puzzle, let us look at the expression of the **critical wavenumber** k_J as given by (8.21). For the early matter-dominated era, if we take $a \propto t^{2/3}$, the Friedmann equation (10.27) gives

$$\rho \approx \frac{1}{6\pi G t^2} \quad (11.37)$$

on **neglecting the curvature term** kc^2/a^2 , which was insignificant at early times. On substituting this for ρ_0 in (8.21), we get

$$k_J^2 = \frac{2}{3c_s^2 t^2}. \quad (11.38)$$

The corresponding Jeans wavelength is

$$\lambda_J = \frac{2\pi}{k_J} = \sqrt{6\pi} c_s t. \quad (11.39)$$

Structure formation

A perturbation would grow only if its wavelength is larger than λ_J .

We now consider the sound speed c_s appearing in (11.39). After the matter-radiation decoupling, it is given by (8.15). Before the formation of atoms, however, a perturbation in matter density would be accompanied by a perturbation in the radiation field which was coupled to matter. Since the pressure of the radiation field is $P = (1/3)\rho c^2$, the sound speed in the radiation field can be as large as

$$c_s = \frac{1}{\sqrt{3}}c.$$

On substituting this in (11.39), we find

$$\lambda_J = \sqrt{2}\pi ct. \tag{11.40}$$

This means that the **Jeans length was even somewhat larger than the horizon size** (of order ct) before matter-radiation decoupling and **then suddenly fell to a much smaller value** given by (11.39) **after the decoupling** when c_s becomes equal to the ordinary sound speed in the gas.

Structure formation

Although perturbations can, in principle, grow after the Universe became matter-dominated, most of the perturbations would have wavelengths smaller than the Jeans length (11.40) and would not grow as long as matter and radiation remained coupled. **Only after the radiation becomes decoupled, does the Jeans length become small and perturbations larger than it start growing.**

We have discussed in §11.5 the possibility that **much of the matter in the Universe is non-baryonic cold dark matter**. If this is true, then the situation can be somewhat tricky.

We expect only the baryonic matter to interact with radiation and to be coupled with it till the formation of atoms. Since the **cold dark matter** can have only the weak interaction, it **must have become decoupled from the other components of the Universe when the temperature fell below MeV values**. By the time the Universe became matter-dominated, the cold dark matter was totally decoupled and **the Jeans length for the cold dark matter would be given by (11.39)**, with c_s representing the sound speed in the cold dark matter. This Jeans length would be **much smaller than the Jeans length of baryonic matter given by (11.40)** before the formation of atoms.

Structure formation

So, as soon as the Universe became matter-dominated and it became possible for perturbations to grow, the perturbations in cold dark matter larger than its Jeans length would start growing. **Eventually, when the atoms form, the baryonic matter also becomes decoupled and its Jeans length drops drastically**, allowing perturbations larger than its Jeans length to grow.

By that time, the **perturbations in the cold dark matter would have grown considerably and would have produced gravitational potential wells in the regions where the cold dark matter got clumped**. Once the baryonic perturbations are allowed to grow after the formation of atoms, **the baryonic matter would quickly fall in the gravitational potential wells created by the cold dark matter**.

Structure formation

Figure 11.7 gives a sketch of how the perturbations must have grown.

When the Universe was **radiation-dominated** till $t = t_{\text{eq}}$, the perturbations in the baryonic matter and the cold dark matter must have had similar amplitudes and **could not grow**.

Since perturbations in the baryonic matter remained frozen till the decoupling time $t = t_{\text{dec}}$ and CMBR observations tell us that the perturbations at the time t_{dec} were of amplitude 10^{-5} , we expect the primordial perturbations also to have this amplitude.

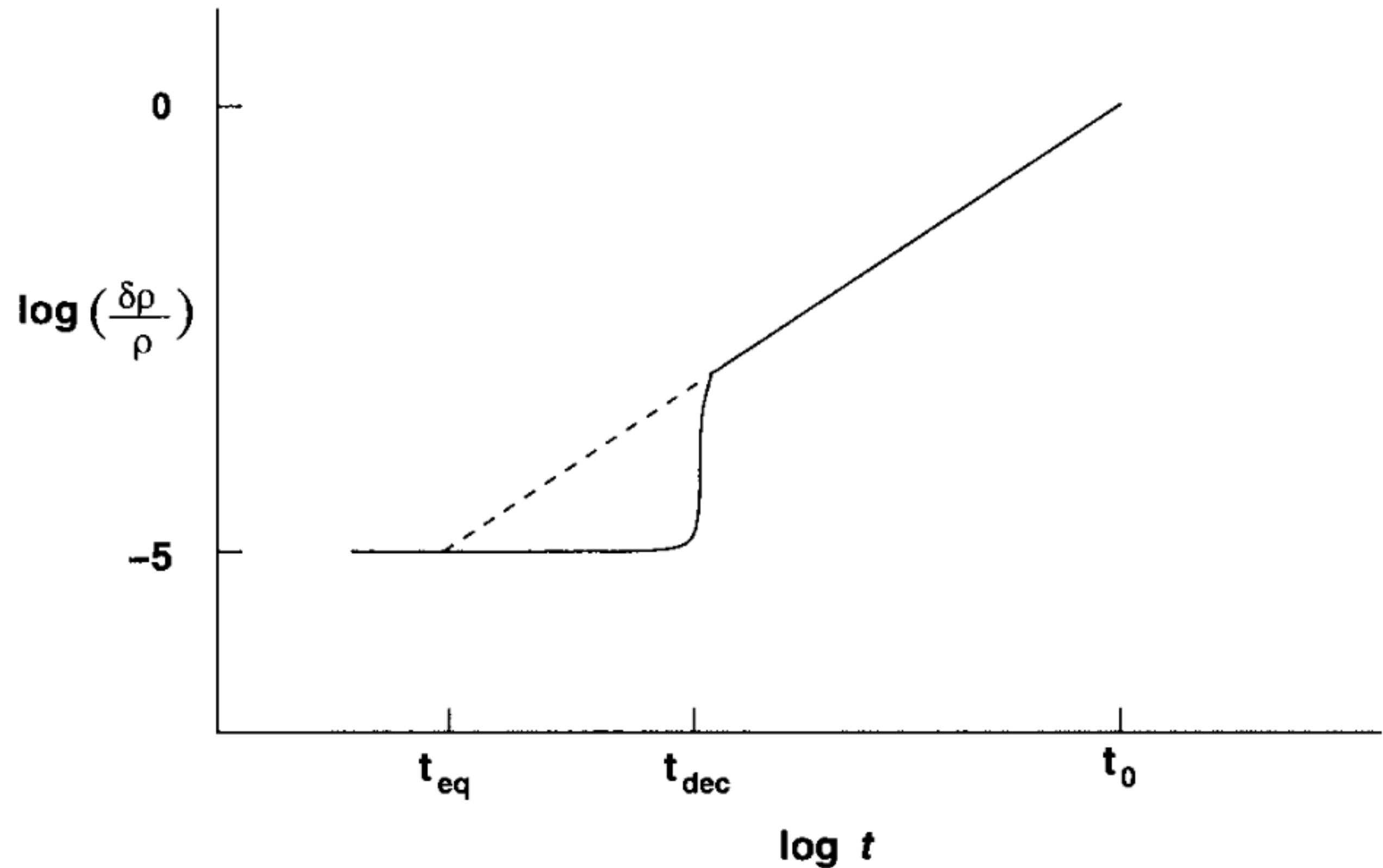


Fig. 11.7 Sketch indicating how perturbations in baryonic matter (solid line) and in cold dark matter (dashed line) would have grown.

Structure formation

Since **cold dark matter perturbations started growing** from $t = t_{\text{eq}}$ when $a = a_{\text{eq}}$ given by (10.52) and the perturbation growth rate is given by (11.36), we expect **the dark matter perturbations to become close to 1 by the present time.**

After $t = t_{\text{dec}}$, the **baryonic perturbations fell in the potential wells of the cold dark matter and started following the cold dark matter perturbations**, as indicated by the solid line in Figure 11.7.

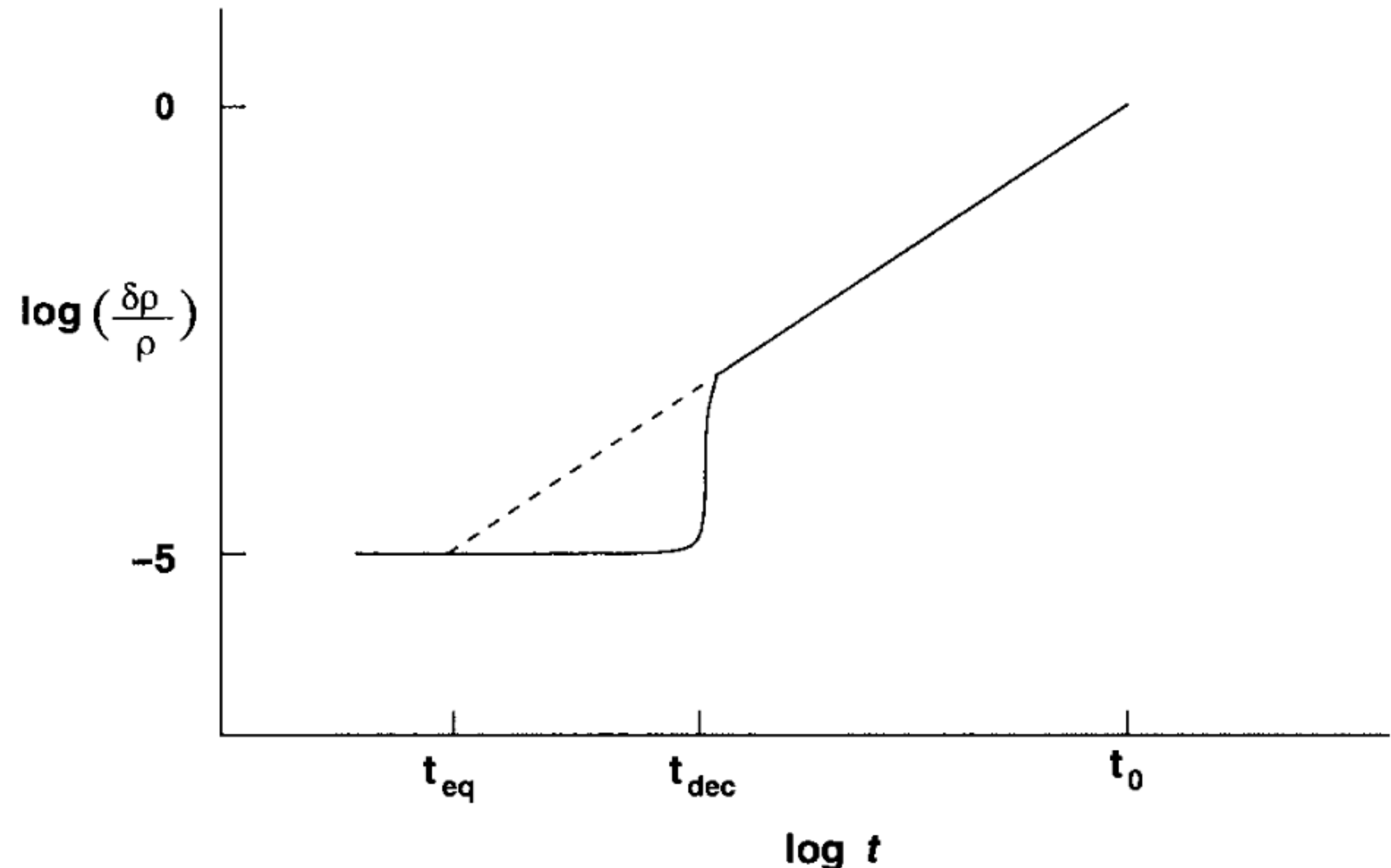


Fig. 11.7 Sketch indicating how perturbations in baryonic matter (solid line) and in cold dark matter (dashed line) would have grown.

Structure formation

Hence the **baryonic perturbations also should become of order 1 by the present time.**

When the perturbations are no longer very small compared to 1, nonlinear effects start becoming important and the clustering of matter to produce various structures proceeds at a much faster rate.

Evolution due to these nonlinear effects can be studied best by carrying on detailed numerical simulations.

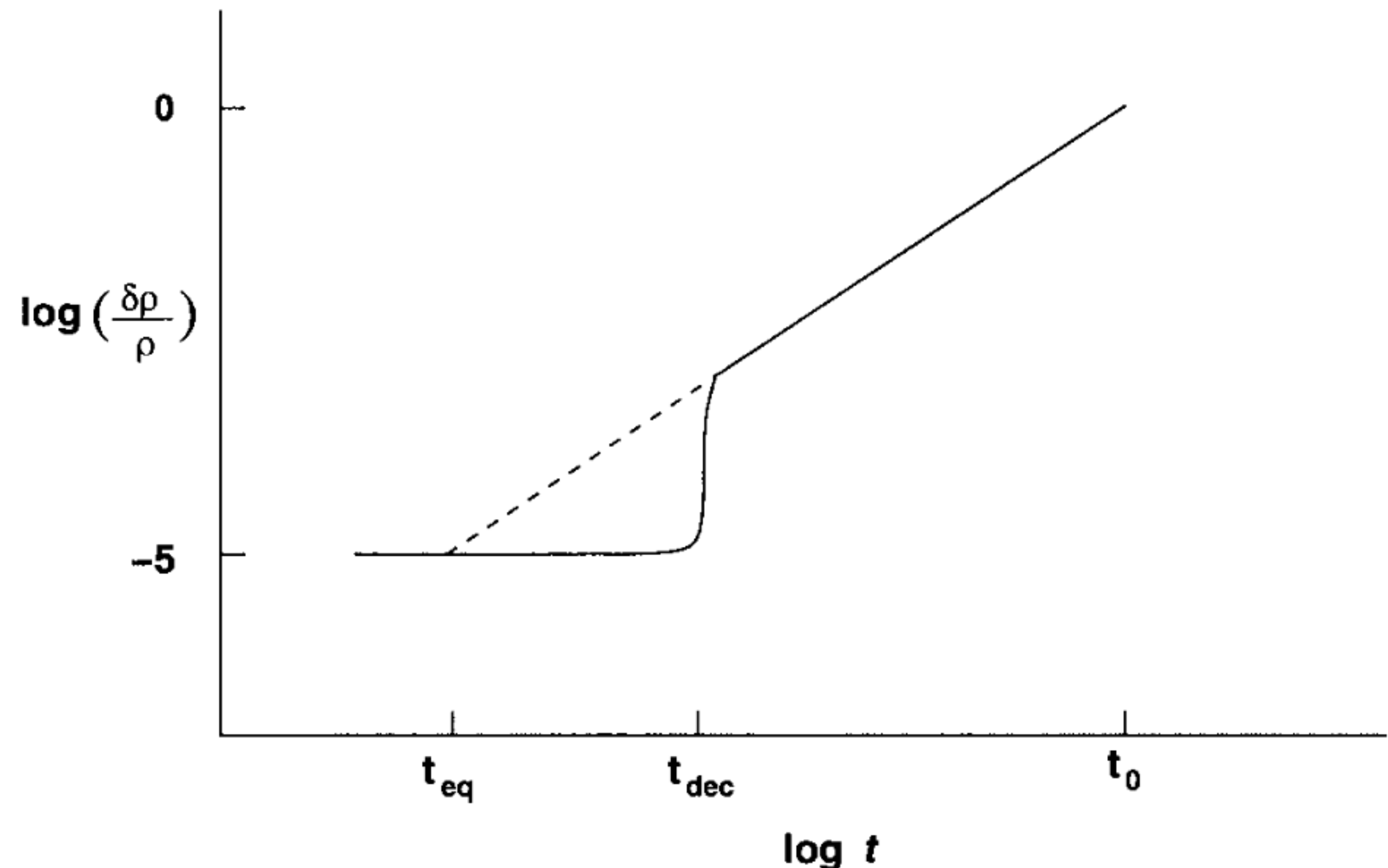


Fig. 11.7 Sketch indicating how perturbations in baryonic matter (solid line) and in cold dark matter (dashed line) would have grown.

Structure formation

Many ambitious numerical simulations of structure formation are being carried out by different groups.

These simulations indicate that structures like what we see today may indeed form if the Universe contains a significant amount of cold dark matter in addition to baryonic matter. This is taken as further compelling evidence that the dark matter in the Universe is cold and not hot. Only if the Universe has a large amount of cold dark matter, would baryonic perturbations having amplitude of order 10^{-5} at t_{dec} be able to grow enough by the present time, by falling in the potential wells created by the cold dark matter, so as to explain the observed structures of today.

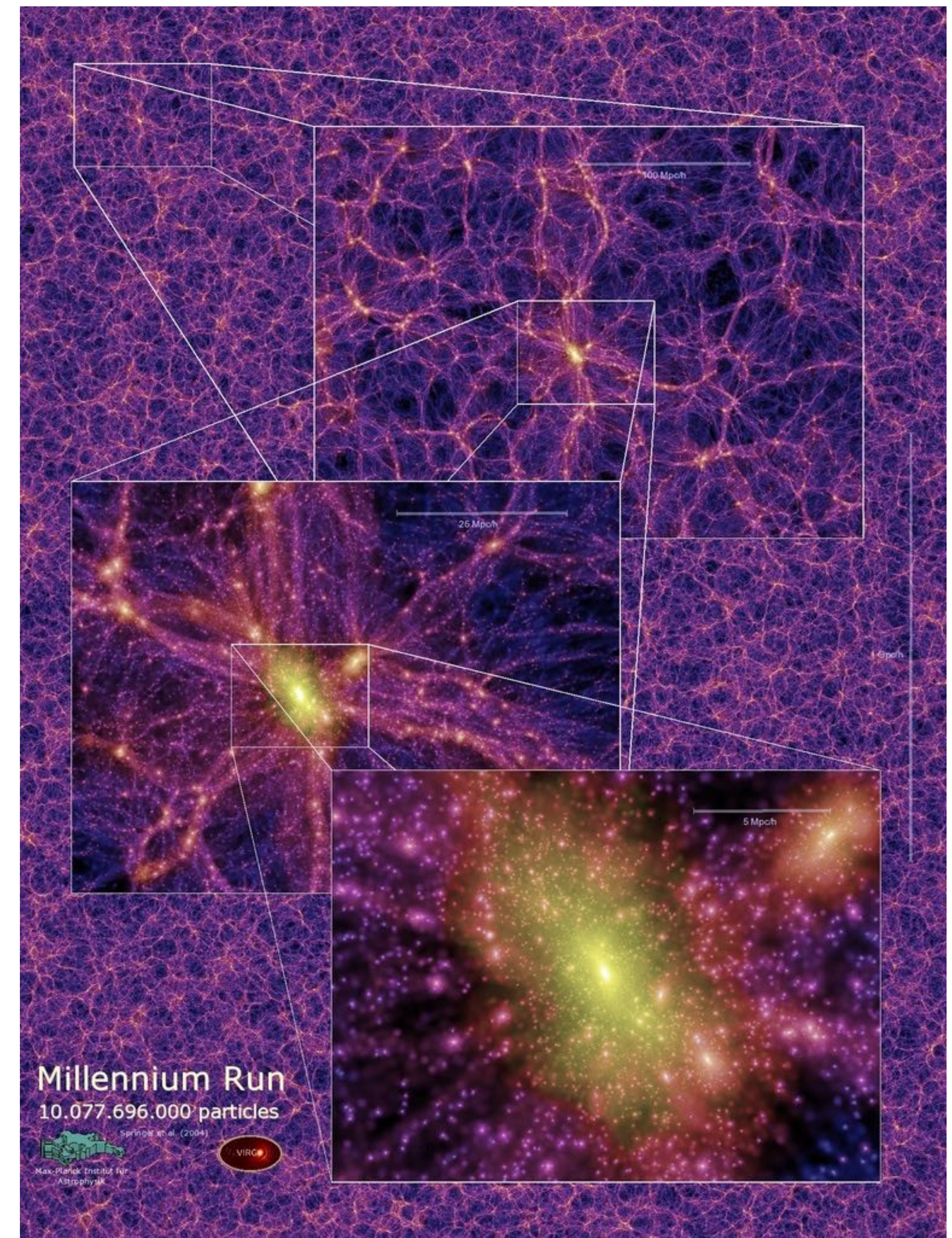
Large scale structure

A slice through the Millennium **simulation** showing the cosmic web of structures. The bright yellow regions are the high density clusters that form at the intersection of filaments.

The Millennium simulation is a **dark matter only** simulation where particles represent mass and interact with other particles only through gravity.

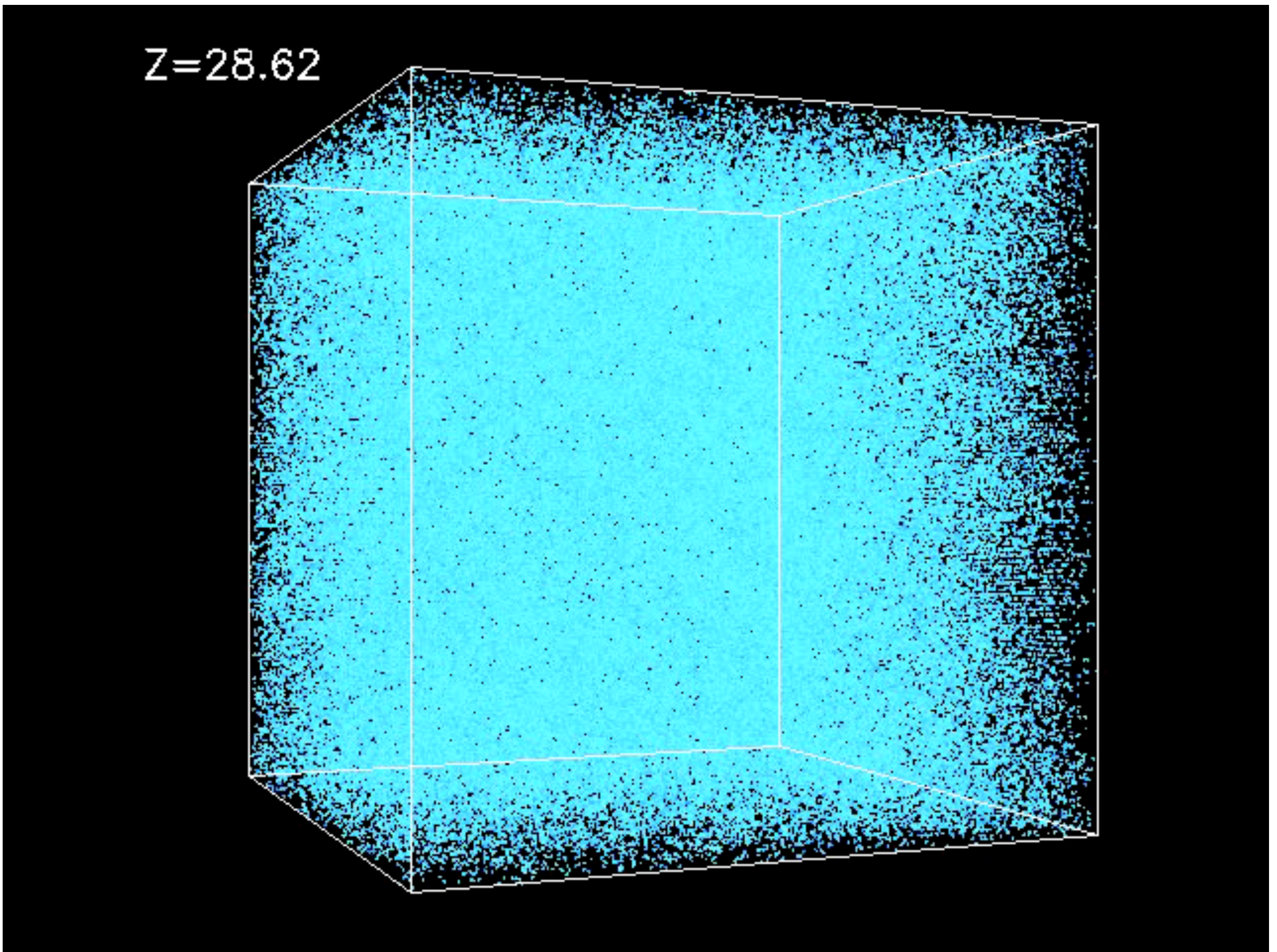
The input is a **matter distribution based on the Cosmic Microwave Background radiation**.

As time passes the dark matter forms the filamentary structure of the Universe that we can observe as the distribution of galaxies.

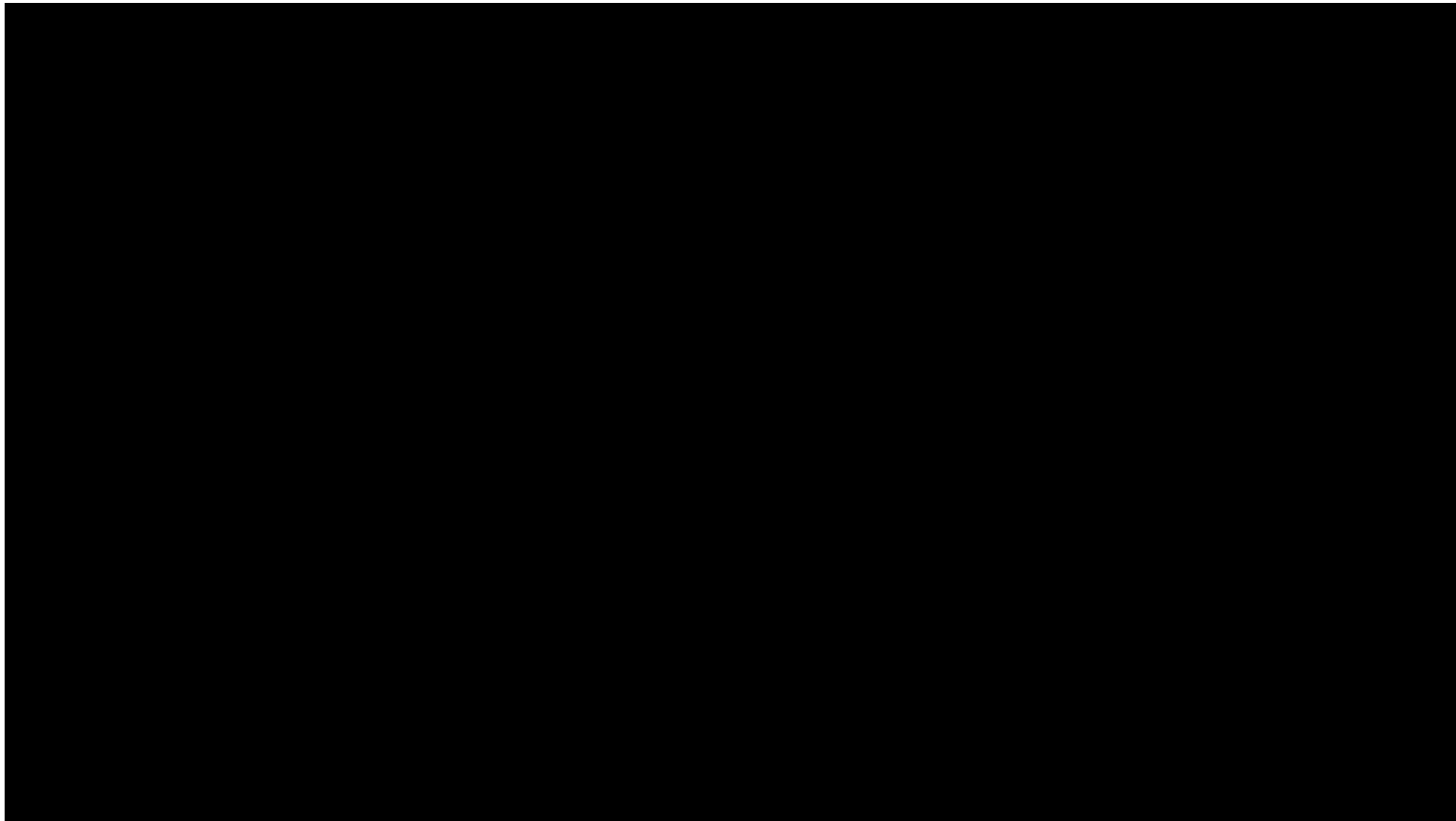


Large scale structure

The movie stills pictured above illustrate the formation of clusters and large-scale filaments in the Cold Dark Matter model with dark energy. The frames show the evolution of structures in a 43 million parsecs (or 140 million light years) box from redshift of 30 to the present epoch (upper left $z=30$ to lower right $z=0$).



Large scale structure



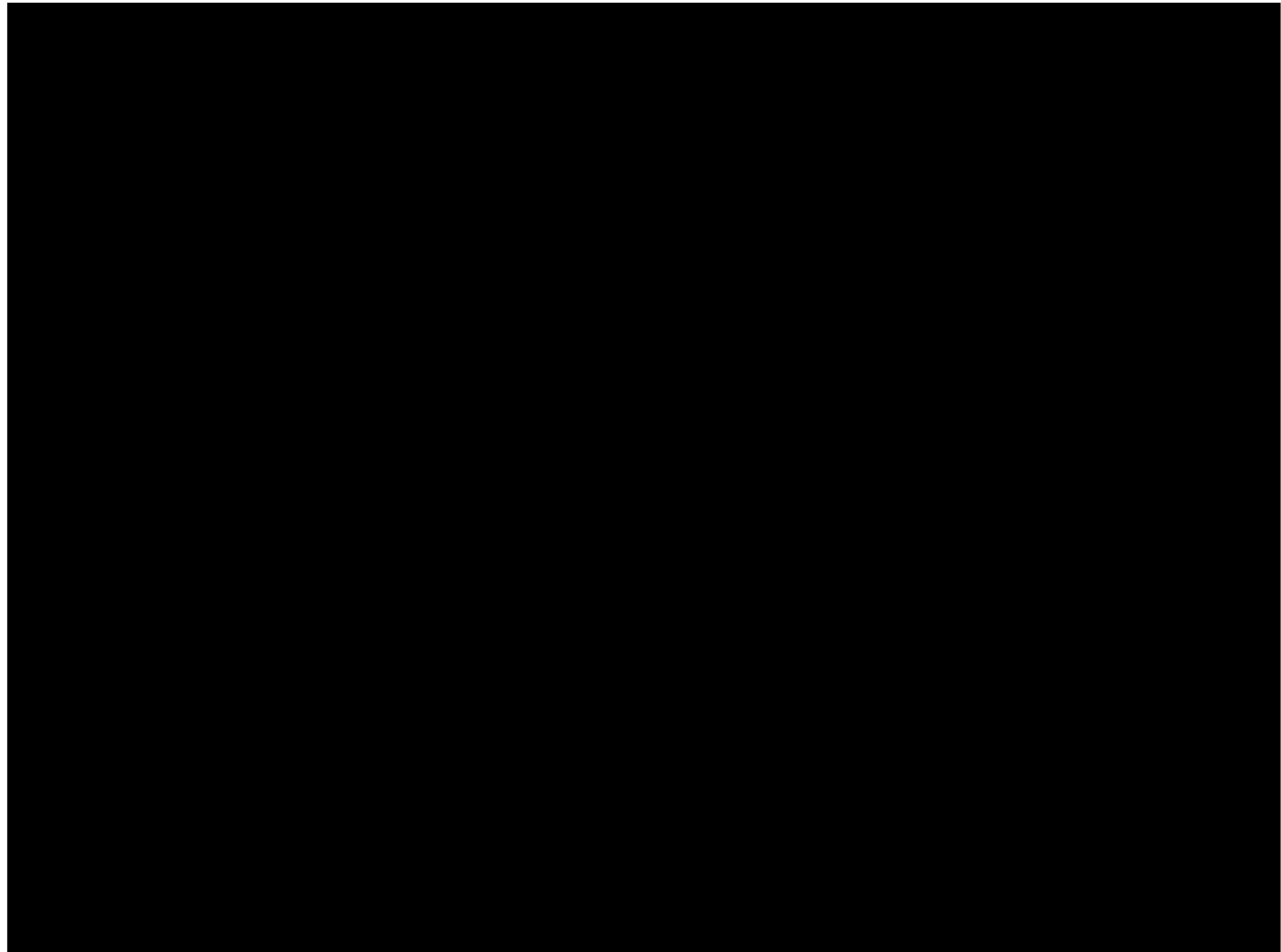
Large scale structure

Cosmological N-body simulation of the formation and evolution of large scale structures in the Universe.

The number of simulated particles is 512^3 .
The size of the simulation box is $\sim 100\text{Mpc}$
(about 300 million light years).

This simulation was carried on Cray XT4 at Center for Computational Astrophysics, CfCA, of National Astronomical Observatory of Japan.

Simulation and Visualization: Tomoaki Ishiyama (University of Tsukuba)



Large scale structure

Cosmological N-body simulation of the formation and evolution of large scale structures in the Universe.

The size of the simulation box is $\sim 1650\text{Mpc}$ (about 5.4 billion light years). This simulation was carried on the K computer at the RIKEN Advanced Institute of Computational Science in Japan.

This simulation offers the highest mass resolution among simulations utilizing boxes larger than $1\text{Gpc}/h$.

Simulations and Visualization: Tomoaki Ishiyama

